Title
Primary and secondary processes in the 193 nm photodissociation of vinyl chloride

Journal
Journal of Chemical Physics, 108(13)

Author
Blank, David A.

Publication Date
1997-12-12

LBNL-41168
UC-401
Preprint

ERNEST ORLANDO LAWRENCE
BERKELEY NATIONAL LABORATORY

Primary and Secondary Processes in the 193 nm Photodissociation of Vinyl Chloride

David A. Blank, Weizhong Sun, Arthur G. Suits,
Yuan T. Lee, Simon W. North, and Gregory E. Hall

Chemical Sciences Division

December 1997

Submitted to
Journal of Chemical Physics

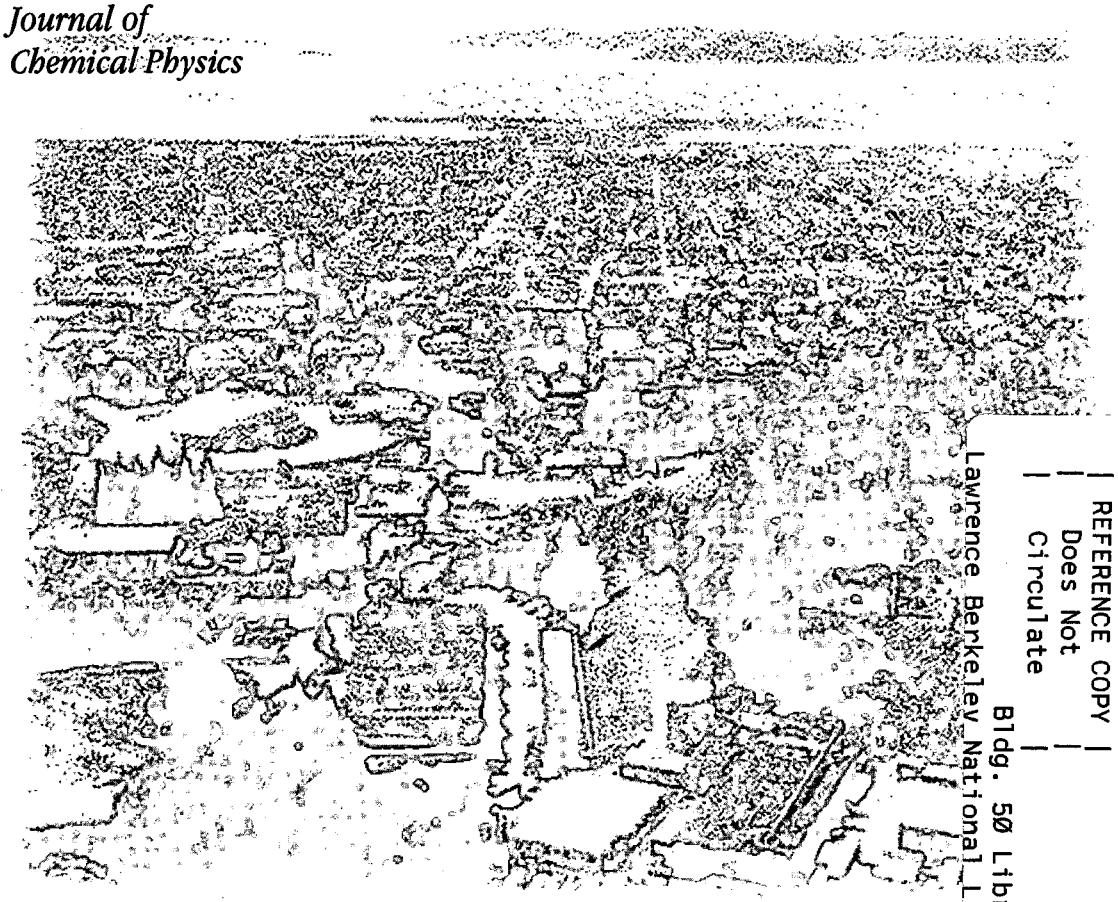

LBNL-41168

DISCLAIMER

LBNL-41168
UC-401

Primary and Secondary Processes in the 193 nm Photodissociation of Vinyl Chloride

David A. Blank, Weizhong Sun, Arthur G. Suits, and Yuan T. Lee

Department of Chemistry
University of California, Berkeley
and
Chemical Sciences Division
Ernest Orlando Lawrence Berkeley National Laboratory
University of California
Berkeley, California 94720

Simon W. North and Gregory E. Hall

Chemistry Department
Brookhaven National Laboratory
Upton, New York 11973-5000

December 1997

This work was supported by the Director, Office of Energy Research, Office of Basic Energy Sciences, Chemical Sciences Division, of the U.S. Department of Energy under Contract No. DE-AC03-76SF00098, and Contract No. DE-AC02-76CH00016.

Primary and secondary processes in the 193 nm photodissociation of vinyl chloride

David A. Blank, Weizhong Sun, Arthur G. Suits, and Yuan T. Lee
Chemical Sciences Division, Lawrence Berkeley Laboratory, University of California, and Chemistry Department, University of California, Berkeley, CA, 94720

Simon W. North[a] and Gregory E. Hall
Chemistry Department, Brookhaven National Laboratory, Upton, NY, 11973-5000

Prepared for J. Chem. Phys. Draft printed 10-Dec-97

Abstract

We have investigated the photodissociation of vinyl chloride (H_2CCHCl) at 193 nm using the technique of photofragment translational spectroscopy. The experiments were performed at the Chemical Dynamics Beamline at the Advanced Light Source and used vacuum ultraviolet synchrotron radiation for product photoionization. We have observed five primary dissociation channels following an initial $\pi^* \leftarrow \pi$ excitation. The majority of Cl atoms originate from an excited-state dissociation. The remaining dissociation channels are consistent with competition on the ground electronic state following internal conversion from the optically prepared state. These channels include atomic and molecular hydrogen elimination, HCl elimination, and a translationally slow Cl elimination channel. We have also identified and characterized two secondary decomposition channels: (1) the elimination of Cl from chlorovinyl radicals following the primary atomic hydrogen elimination channel, and (2) hydrogen atom elimination from vinyl radicals following the primary atomic Cl elimination. By measuring the truncation

---

[a] Present address: Department of Chemistry, Texas A&M University, college Station, TX, 77843.

in the translational energy distribution for C_2H_2Cl products from primary atomic hydrogen elimination we deduce a barrier for the reverse reaction of Cl + acetylene of 11 ± 2 kcal/mol. Since Cl is known to add rapidly to acetylene with no activation barrier, we conclude that H loss primarily forms the $ClCCH_2$ isomer, and that the observed 11 kcal/mol barrier pertains to a concerted addition/rearrangement path to form the α–chlorovinyl radical. Finally, we report low-resolution photoionization spectra for the nascent vinyl radical and HCl photoproducts, in which red shifts in the ionization onsets can be related to the internal energy content.

1. Introduction

The ultraviolet photodissociation of chloroethylenes remains the object of active interest, even after decades of study. The general goal has been to understand the effects of substitution on multiple open channels in the photochemistry of small, unsaturated hydrocarbons. The ultraviolet absorption in these molecules is characterized by a strong band near 190 nm dominated by a $\pi^* \leftarrow \pi$ transition. At wavelengths <200 nm there is sufficient energy for several dissociation pathways to compete. The elimination of HCl, H_2, H, and $Cl(^2P_J)$ have all been identified as primary dissociation processes in the 193 nm photodissociation of vinyl chloride. Figure 1 shows the relative energetics and estimated barrier heights of these channels.

Extensive vibrational excitation in the HCl channel was demonstrated in photochemical laser studies with broad-band photolysis at wavelengths λ>155 nm.[1] Infrared emission spectroscopy by Moss *et al.* found substantial vibrational excitation in the acetylene/chloroacetylene partner fragments and a high degree of rotational excitation in the HCl products.[2] Donaldson and Leone[3] used FTIR emission spectroscopy following photolysis at 193 nm to measure nascent HCl vibrational distributions in general agreement with results from the broadband chemical laser experiments. Photofragment

translational spectroscopy (PTS) experiments on the 193 nm photodissociation of chloroethylenes measured non-statistical translational energy distributions for HCl photoproducts.[4] The HCl fragments exhibited little velocity anisotropy, suggesting that internal conversion from the initially excited electronic state preceded dissociation. A series of resonance-enhanced multiphoton ionization (REMPI) spectroscopic studies[5,6,7,8,9,10,11] of the HCl photofragments from laser photodissociation of chloroethylenes has revealed an unusual pattern of state distributions with surprisingly little dependence on the precursor. The HCl (v = 0) rotational distribution could be characterized with a superposition of two temperatures, while the distributions for HCl (v > 0) could be well represented by a single, high temperature. Remarkably, very similar HCl state distributions were observed for vinyl chloride,[5] d_1-vinyl chloride,[8] and all three isomeric dichloroethenes[7] at 193 nm, as well as at longer wavelengths.[11] Relative quantum yields for HCl from these precursors were remeasured, and significant differences were found compared to earlier chemical laser experiments.[1] HCl yields deduced from chemical laser experiments had led Berry[1] to conclude that HCl loss in chloroethenes occurred predominantly *via* a 1,2 elimination mechanism. The interpretation of isomeric and isotopic studies of the chloroethylenes has always been complicated by the energy-dependent competition of fragmentation with both cis-trans isomerization and 1,2 shift isomerization.[8,12,13] The REMPI measurements of Gordon and co-workers were originally interpreted as a 3:1 preference for 1,1 over 1,2 elimination in vinyl chloride.[8] Following state-resolved translational energy measurements[9,10] and theoretical studies of the vinyl chloride[14] and dichloroethylene[15] ground state surfaces, the most recent proposal[10] is that 1,2 hydrogen migration occurs in competition with 1,1 HCl elimination, with no significant contribution from 1,2 elimination. The substantial HCl vibrational and translational energy is explained by noting that the isomerization of vinylidene to acetylene can be rapid enough to be considered as part of a concerted process, sharing the C_2H_2 isomerization energy with the HCl.

The elimination of Cl atoms from all the chloroethylenes results in a bimodal translational energy distribution.[4,6,9,10,16,17] A fast and anisotropic Cl fragment channel, dominant in the photodissociation of vinyl chloride, has been attributed to dissociation on a repulsive potential energy surface. The optically prepared ($\pi\pi^*$) bound state has generally been thought to be predissociated by the repulsive $n\sigma^*_{(C\text{-}Cl)}$ state, although reassignment to a $\pi(Cl)\sigma^*_{(C\text{-}Cl)}$ dissociative state has been recently suggested.[17] A slower Cl channel has been attributed to internal conversion followed by dissociation on the electronic ground state. The Cl fine structure branching favors the $Cl(^2P_{3/2})$ spin orbit ground state in both fast and slow channels, although quantitative differences exist between published measurements,[10, 17] evidently due in part to different background correction schemes used in the REMPI Doppler and ion imaging experiments.

Gordon and co-workers have measured Doppler profiles for hydrogen atom products that were consistent with Boltzmann distributions containing 25%-33% of the available energy.[6] They also measured nascent rotational state distributions for H_2 photoproducts in the first 5 vibrational levels and extracted the average translational energy release for two rovibrational states.[18]

Reihl and Morokuma have investigated the dissociation of the chloroethylenes using *ab initio* molecular orbital methods.[14,15] The authors calculated asymptotic energies and transition states for all dissociation pathways, including barriers to isomerization. The 1,1 HCl elimination channel was predicted to have a lower barrier to dissociation than 1,2 elimination, in agreement with experimental work of Gordon and co-workers.[6] The barrier to H atom migration was determined to be slightly below the 1,1 HCl elimination barrier, suggesting that partial H atom scrambling may precede dissociation. The authors also concluded that 1,1 HCl elimination would exceed the loss of H_2 since the barrier to H_2 elimination is 30 kcal/mol higher in energy. The vinylidene/chlorovinylidene products formed following 1,1 elimination of either HCl or H_2 were calculated to have a very small barrier to H atom migration, indicating rapid isomerization to acetylene/chloroacetylene. The calculated endothermicity of atomic H

and Cl elimination was close to the barrier for 1,1 H_2 elimination. Elimination of an H atom from the α carbon was determined to be favored over loss from the β carbon, in contrast to the inferences of Gordon and co-workers.[6]

Although there is sufficient energy near 200 nm to enable the subsequent dissociation of primary fragments, the importance of these secondary processes has not been considered until very recently. In a recent PTS study of the ultraviolet photodissociation of chloroethylenes,[19] Sato *et al.* reported that a contribution from the secondary decomposition of the chlorovinyl radical was necessary to obtain satisfactory fits to the Cl^+ and $C_2H_2^+$ time of flight (TOF) data. The derived translational energy distribution, $P(E_T)$, for secondary C-Cl bond cleavage was peaked away from zero and interpreted as the result of a substantial centrifugal barrier to dissociation. Suzuki and co-workers have observed an increase in the $Cl(^2P_{3/2})/Cl(^2P_{1/2})$ ratio in the low velocity Cl channel from vinyl chloride when the dissociation wavelength was decreased from 210 nm to 193 nm.[17] Expecting more adiabatic formation of $Cl(^2P_{3/2})$ from the low energy secondary dissociation, these authors attribute the energy-dependent fine structure branching ratio to partial secondary decomposition of C_2H_2Cl intermediates, citing consistency with the PTS work by Sato *et al.*,[19] and a preliminary report of the present work.

In this investigation we have used the technique of photofragment translational spectroscopy with tunable vacuum ultraviolet product photoionization to study the dissociation of vinyl chloride at 193 nm. We have recently applied the same methods to the photodissociation dynamics of the analogous molecule acrylonitrile.[20] We have measured state averaged center-of-mass translational energy distributions for the primary HCl, Cl, and H_2 elimination channels at higher resolution than previously reported. We also report the first direct measurements of the secondary decomposition of both vinyl and chlorovinyl radical primary dissociation products. The secondary decomposition of primary vinyl radical photoproducts is evident through comparison of the measured $P(E_T)$ for the Cl and momentum matched vinyl radical fragments. Secondary decomposition of

the chlorovinyl radicals exhibits itself as an abrupt truncation in the measured $P(E_T)$ for chlorovinyl radicals. The truncation and secondary $P(E_T)$ suggest that primary H loss preferentially produces the α-chlorovinyl radical, and that there is a substantial recombination barrier to form the α-chlorovinyl radical from Cl and acetylene. The identification and characterization of the secondary decomposition channels is essential for a sensible interpretation of observed branching ratios in the chloroethylenes. Finally, we report low-resolution photoionization spectra for the vinyl radical and HCl photoproducts.

2. Experimental

The fixed detector-rotating source molecular beam apparatus as been described in detail elsewhere.[21] A continuous molecular beam of 4.5% vinyl chloride seeded in helium was skimmed twice and intersected at 90° with the output of a Lambda Physik LPX-200 excimer laser operating on the ArF transition (193.3 nm). There was no change in the shape of any of the TOF spectra over a laser fluence range of 30-300 mJ/cm^2 providing strong evidence that all of the observed signals are the result of single photon absorption.[22] Previous intensity-dependent measurements on vinyl chloride at 193 nm by Gordon and co-workers[6,18] have reported no deviations from a linear power dependence for H atoms and H_2 up to 150 mJ/cm^2, HCl up to 40 mJ/cm^2, and Cl atoms up to 15 mJ/cm^2. The TOF spectra presented were taken with a laser fluence of ~100 mJ/cm^2. Neutral photodissociation products traveled 15.1 cm where they were ionized by tunable VUV undulator radiation, mass selected, and counted as a function of time.

The characteristics of the VUV undulator radiation used for product photoionization have also been previously described.[23] Briefly, the VUV radiation was focussed to 150 μm x 250 μm at the point of intersection with the scattered neutral photodissociation products. The flux of the undulator radiation, typically $1x10^{16}$

photon/sec, was continuously monitored using a VUV calorimeter. For measurements of the photoionization onsets of photodissociation products the total scattering signal at a fixed source angle was integrated as the undulator energy was stepped.

Vinyl chloride 99.5% was obtained from Aldrich Chemical Co. and used without further purification.

3. Results

For all of the time of flight (TOF) spectra presented the circles represent the raw data, the dashed lines are single channel contributions to the forward convolution fit, and the solid lines are the combined overall fit to the data. The photodissociation laser was unpolarized in all of the experiments presented here, which results in an isotropic laboratory photofragment distribution in the plane defined by the molecular beam and detector axis. Center of mass translational energy distributions, $P(E_T)$, were obtained from the time of flight spectra, TOF, using the forward convolution technique.[24,25] The forward convolution technique involves convolution of a trial $P(E_T)$ and photofragment angular distribution, $T(\theta)$, over the instrument response function to generate a simulated TOF spectrum. The simulated TOF spectrum is then compared to the experimental data and the $P(E_T)$ and $T(\theta)$ are iteratively adjusted until a best fit to the data is obtained. When detecting chlorine-containing products it is possible to select a single isotope. It is not possible, however, to specify the isotopomer when the chlorine containing product is the 'unseen' momentum matched partner fragment. In such cases the forward convolution fits represent the weighted sum of fits for each isotopomer.

Atomic hydrogen elimination and secondary decomposition of chlorovinyl intermediates. The TOF spectrum for m/e 61 ($C_2H_2Cl^+$) at a scattering angle of 7.0° and a photoionization energy of 11.0 eV is shown in Figure 2. The TOF spectrum was fitted with the $P(E_T)$ in Figure 3. Assuming that the internal energy in the vinyl chloride reactant is negligible[26], $E_{h\nu}$ =148 kcal/mol, and $D_0(H\text{-}C_2H_2Cl)$ = 101 kcal/mol (ref 27) there is 47 kcal/mol of available energy following H atom elimination. The $P(E_T)$

decreases out to the maximum available energy and exhibits an sharp cut-off at 11 kcal/mol. Since there is insufficient energy for electronic excitation of the departing hydrogen atom, any available energy not partitioned into product translation will be distributed among the internal degrees of freedom of the chlorovinyl radical. Our measured $P(E_T)$, therefore, provides a measure of the internal energy distribution in the chlorovinyl photoproducts. An abrupt truncation of a primary $P(E_T)$ generally indicates the secondary decomposition of an intermediate species with sufficient internal energy to dissociate prior to detection. The solid lines in Figures 2 and 3 represent the best fit to the data and the dashed lines demonstrate the sensitivity (±2 kcal/mol) of the forward convolution fit to the position of truncation in the $P(E_T)$. The only energetically accessible secondary decomposition pathway for the chlorovinyl radicals is C-Cl bond cleavage to give acetylene and a chlorine atom. Figure 4 shows a schematic representation of the relationship between the truncation in the primary $P(E_T)$ for H atom elimination and the barrier to secondary C-Cl bond cleavage in chlorovinyl radical photoproducts. A truncation of the $P(E_T)$ at 11±2 kcal/mol corresponds to a dissociation barrier of 36±2 kcal/mol for C-Cl bond cleavage in the chlorovinyl radical, which exceeds the reaction endothermicity by 11 kcal/mol.[27] The statistical elimination of a hydrogen atom generates very little torque on the C_2H_2Cl fragment precluding rotational metastability of the C_2H_2Cl from influencing the determination of the dissociation barrier height.

As a result of the secondary decomposition of chlorovinyl products, we are unable to measure the $P(E_T)$ for the H-atom elimination channel below 11 kcal/mol by detecting the m/e 61 photofragments. Measurements at m/e 1 and 2 are experimentally more difficult than at higher masses, and were not performed in the course of this work.

Molecular hydrogen elimination. Figure 5 shows TOF spectra for m/e 60 (C_2HCl^+) at scattering angles of 10° and 15° and a photoionization energy of 12.0 eV. The dominant component in the 10° spectrum and the only component in the 15° spectrum is the result of H_2 elimination and was fitted the $P(E_T)$ shown in Figure 6. The

$P(E_T)$ in Figure 6 has a near Gaussian shape with $<E_T>$ = 18±2 kcal/mol and a FWHM of ~20 kcal/mol. The minor component in the 10° spectrum arises from dissociative photoionization of C_2H_2Cl photoproducts and was fitted with the $P(E_T)$ in Figure 3 for H atom elimination.

HCl elimination. The TOF spectra for m/e 36 ($H^{35}Cl^+$) at scattering angles of 20° and 40° and a photoionization energy of 14.0 eV are shown in Figure 7. The TOF spectra in Figure 7 were fitted with the $P(E_T)$ in Figure 8 which has a maximum probability at 12 kcal/mol and extends to ~70 kcal/mol. The measured distribution has an average value of 18 ± 1 kcal/mol. The photoionization spectrum for m/e 36 photoproducts at a scattering angle of 20° is shown in Figure 9. Accounting for the energy width of the undulator radiation, the HCl fragment photoionization onset is 10.5 ± 0.3 eV. Comparison of this value with the HCl ionization potential (IP) of 12.75 eV (ref. 28) demonstrates a red shift of ~2.2 eV in the photoionization onset. The red shift reflects the influence of internal excitation on HCl photoionization. At present, the quantitative extraction of fragment internal energy from a measured photoionization spectrum is an unsolved problem. A qualitative discussion of the internal energy in the HCl photofragments from the reduction of the photoionization onset is presented below.

Atomic chlorine elimination and secondary decomposition of the vinyl radical intermediates. The TOF spectra for m/e 27 ($C_2H_3^+$) at scattering angles of 15° and 25° and a photoionization energy of 11.0 eV are shown in Figure 10. Vinyl radicals can only originate from primary C-Cl bond cleavage and have been fitted with the $P(E_T)$ in Figure 11 assuming Cl (mass 35 and 37) as the momentum matched partner fragment. The $P(E_T)$ is nearly Gaussian with an average energy of 23±1 kcal/mol. The TOF spectrum for m/e 35 ($^{35}Cl^+$) at a scattering angle of 7° and a photoionization energy of 14.0 eV is shown in Figure 12. The TOF spectrum has been fitted with two components, represented by the dashed lines. The narrow component at earlier times was fitted with the $P(E_T)$ in Figure 11 derived from fitting the vinyl radical TOF spectra. The remaining slow component in m/e 35 TOF spectrum was fitted with the $P(E_T)$ in Figure 13. Note that the $P(E_T)$ in

Figure 13 is the translational energy distribution of Cl products and *not the total* translational energy distribution reported in all of the other figures presented in this manuscript. The $P(E_T)$ exhibits a maximum probability at ~0.5 kcal/mol, decreasing to a plateau from 2-4 kcal/mol, and then decreases out to a maximum energy of ~7 kcal/mol. The complex shape suggests that the $P(E_T)$ in Figure 13 contains contributions from at least two components.

We can further decompose the $P(E_T)$ for the slow Cl photofragments shown in Figure 13 into two dissociation channels. We have assigned the slower portion of the $P(E_T)$ to statistical C-Cl bond cleavage channel, $H_2CCHCl \rightarrow H_2CCH + Cl$, using an adjustable available energy in the functional form of the prior translational energy. The optimized $P(E_T)$ for this channel is shown as the solid line in the top of Figure 14. The contribution of this channel to TOF spectra can be seen most clearly in Figure 15 as the broad peak at 120 μsecs. Inspection of Figure 10 shows that the translationally slow Cl atoms have no momentum-matched vinyl radicals. The missing slow vinyl radicals in Figure 10 are evidence of secondary decomposition of the vinyl radical intermediates produced in the translationally slow Cl elimination channel, $C_2H_3^{\ddagger} \rightarrow C_2H_2 + H$.

The remaining region of the $P(E_T)$ in Figure 13 we attribute to secondary C-Cl bond cleavage in the chlorovinyl intermediates following primary H atom elimination. Initial evidence for this secondary channel was provided by the truncation in the $P(E_T)$ required to fit the C_2H_2Cl TOF spectra. The dashed line in the lower panel of Figure 14 is the $P(E_T)$ for the primary H atom elimination channel. The low energy portion of the primary $P(E_T)$ for the H atom elimination is not directly observed, due the secondary decomposition of $C_2H_2Cl^{\ddagger}$ intermediates. We assume, however, that the $P(E_T)$ below 11 kcal/mol is similar to the measured $P(E_T)$ for the H atom elimination channel in ethylene.[29] As a result of the large difference in the masses, the $C_2H_2Cl^{\ddagger}$ fragments from the primary dissociation step receive very little recoil velocity, and the forward convolution fits are relatively insensitive to the choice of the $P(E_T)$ used to represent the primary H atom elimination channel. The fits are, however, very sensitive to the $P(E_T)$

for secondary decomposition of the $C_2H_2Cl^‡$ intermediates. The solid line in the lower panel of Figure 14 is the $P(E_T)$ for the secondary decomposition of the chlorovinyl radical intermediates, $C_2H_2Cl^‡ \rightarrow C_2H_2 + Cl$. The resulting fits to the TOF data are shown in Figure 15. The secondary $P(E_T)$ has a maximum probability at ~8 kcal/mol, which is consistent with the measured recombination barrier for the secondary decomposition process of 11±2 kcal/mol, assuming a significant fraction of the exit barrier potential energy is partitioned into fragment recoil.[30] A secondary angular distribution with forward-backward symmetry was used in the forward convolution fitting.[31,32]

We have obtained the branching ratio for the three atomic chlorine elimination channels that contribute to the TOF data in Figure 15. The translationally fast primary Cl elimination channel accounts for 0.86 of the total Cl produced. The translationally slow primary Cl elimination channel accounts for 0.07 of the Cl photoproducts, and the secondary decomposition of chlorovinyl intermediates accounts for the remaining 0.07 of Cl photoproducts. We estimate that the errors associated with these values are less than ±0.02. None of the fast vinyl radicals and all of the slow vinyl radicals undergo secondary dissociation, so this Cl branching distribution provides a direct calibration of the primary H atom yield relative to the primary Cl yield, and a good estimate of the ratio of primary and secondary H atoms.

The photoionization spectrum for m/e 27 ($C_2H_3^+$) photoproducts at a scattering angle of 20° is shown in Figure 16. Stable vinyl radical photoproducts are only formed in coincidence with the translationally fast fragments. Taking into consideration the energy width of the ALS photoionization beam, Figure 16 shows a photoionization onset of 8.3±0.3 eV. This spectrum is consistent with published high-resolution photoionization spectra of vinyl radicals,[33] which show an ionization onset at 8.59 eV for room temperature samples, decreasing to 8.43 eV at around 1200 K.

Photoproducts at m/e 26. TOF spectra for m/e 26 ($C_2H_2^+$) at scattering angles of 10° and 20° at a photoionization energy of 14.0 eV are shown in Figure 17. There are

three dissociation channels, previously identified, which will result in the production of C_2H_2 photoproducts, reactions 1-3:

$$H_2CCHCl \rightarrow HCl + C_2H_2 \qquad \text{(rxn 1)}$$

$$H_2CCHCl \rightarrow C_2H_3^{\ddagger} + Cl \rightarrow C_2H_2 + H + Cl \qquad \text{(rxn 2)}$$

$$H_2CCHCl \rightarrow C_2H_2Cl^{\ddagger} + H \rightarrow C_2H_2 + Cl + H \qquad \text{(rxn 3)}$$

The forward convolution fits to the two TOF spectra at 14 eV include contributions from all three of these dissociation channels. In order to simulate the secondary decomposition of the vinyl radical intermediates, the second step in reaction 2, we assumed a prior translational energy distribution consistent with statistical simple bond rupture. The large difference in the masses of the products from the second step in reaction 2 results in negligible c.m. velocity imparted to the C_2H_2 fragment and the forward convolution fit is relatively insensitive to the shape of this $P(E_T)$. A secondary angular distribution with forward-backward symmetry, consistent with a stepwise dissociation mechanism, was used in the fitting.

In addition to reactions 1-3, it was also necessary to include a contribution to the m/e 26 TOF spectra from dissociative ionization of C_2H_3 photofragments formed in coincidence with translationally fast Cl atoms. This narrow contribution, peaked ~50 μsecs in the m/e 26 TOF spectra, was derived from the $P(E_T)$ in Figure 11. The requirement that reactions 2 and 3 be included to obtain a satisfactory fit to the TOF spectra provides an important confirmation of these two secondary decomposition processes.

The m/e 26 TOF spectrum at a scattering angle of 10° and at a photoionization energy of 11.0 eV is shown in the bottom panel of Figure 17. The TOF spectrum is only composed of contributions from reaction 1 and the dissociative ionization of C_2H_3 products. Reducing the photoionization energy from 14 eV to 11 eV, below the 11.4 eV I.P. of acetylene, removes the signal from acetylene products without significant internal

energy. The absence of contributions from reactions 2 and 3 in the TOF spectrum at 11.0 eV demonstrates that the C_2H_2 products from these reactions contain far less internal energy than the C_2H_2 products from reaction 1. This is consistent with the substantially higher asymptotic energies of these two channels compared to reaction 1. The ability to discriminate between dissociation channels that form products with the identical chemical identity but which result from different dissociation mechanisms is another significant advantage of this technique over traditional PTS experiments that employ electron impact ionization for detection.[20,34]

4. Discussion

A. Molecular Elimination Channels

HCl elimination. The photoionization spectrum for the HCl photoproducts, shown in Figure 9, has an onset which is red shifted from the HCl IP by ~2.2 eV. We have previously observed that the red shift of the photoionization onset provides a qualitative indication of the degree of internal energy in the photofragments.[20,22,34] The magnitude of the red shift suggests that a significant fraction of the available energy is partitioned into rotation and vibration of the HCl photoproducts. The large internal excitation we observe is consistent with more detailed spectroscopic results.[1,2,3,5]

The measured $P(E_T)$ for the HCl elimination channel is qualitatively similar to the result of Umemoto *et al.*[4] using traditional PTS techniques at a fixed scattering angle of 90°. However, our distribution has a higher average translational energy, $\langle E_T \rangle = 18 \pm 1$ kcal/mol compared to $\langle E_T \rangle = 15 \pm 1$ kcal/mol, presumably due to the high energy tail of our $P(E_T)$ which extends almost 10 kcal/mol beyond the maximum of the earlier measurement. Unfortunately Umemoto *et al.* did not report either the laser fluence or the molecular beam conditions employed in their experiments, precluding an assessment of the importance of multiphoton effects or clusters in their work. Our derived $P(E_T)$ is also in good agreement with the Doppler measurements of Huang *et al.*,[10] which show the

state selected velocity distributions narrowing and shifting toward lower energy with increasing HCl vibrational excitation. Their measured average translational energies range 25 ± 2 kcal/mol for HCl (v=0) to 18 ± 1 kcal/mol for HCl (v=2). Assuming that the trend continues with increasing HCl vibrational levels, the substantial population of v>2 states measured by other workers[1,3] should result in an average translational energy that is close to our measured value.

Energetically there are three C_2H_2 isomers that can be formed from the elimination of HCl, reactions 4-6.

$$H_2CCHCl \rightarrow HCl + HCCH \qquad \Delta H_0 = 24 \text{ kcal/mol} \qquad \text{(rxn 4)}$$

$$H_2CCHCl \rightarrow HCl + :CCH_2\ (^1A_1) \qquad \Delta H_0 = 67 \text{ kcal/mol} \qquad \text{(rxn 5)}$$

$$H_2CCHCl \rightarrow HCl + :CCH_2\ (^3B_2) \qquad \Delta H_0 = 113 \text{ kcal/mol} \qquad \text{(rxn 6)}$$

Energy conservation and our measured $P(E_T)$ cannot alone rule out reaction 6, since there is significant probability below the 45 kcal/mol available energy for this channel. There is, however, no break in the distribution at the threshold, and given the extensive rovibrational energy of HCl, the involvement of reaction 6 appears unlikely at 193 nm.

The calculated recombination barriers for reactions 4 and 5 are 63 kcal/mol and 3 kcal/mol respectively.[14] The small recombination barrier for 1,1 elimination should result in a near statistical translational energy release with a maximum probability <3 kcal/mol. The 12-13 kcal/mol maximum in our measured $P(E_T)$ suggests a larger recombination barrier such as that calculated for reaction 4. The present measurements are consistent with the most recent explanations of Gordon and co-workers,[10] based on the *ab initio* calculations of Riehl and Morokuma.[14] The large translational energy release is thought to arise from isomerization of singlet vinylidene to acetylene on a time scale comparable to the separation of the two photofragments. Lineberger and co-workers have estimated the lifetime of singlet vinylidene at 40-200 fs from linewidth analysis of negative ion photodetachment experiments.[35] This is consistent with the calculated barrier to

isomerization of singlet vinylidene to acetylene of 2-4 kcal/mol.[36] A concerted isomerization/dissociation mechanism would allow a fraction of the energy of isomerization to be available to degrees of freedom other than internal energy of the C_2H_2 fragment. The rapid isomerization of vinylidene would leave acetylene and HCl in close proximity and the repulsive interaction could provide the additional translational energy release observed.

Molecular hydrogen elimination. The present study represents the first state averaged measurement of $P(E_T)$ for this dissociation channel. Where they can be compared, the present results are in good agreement with the Doppler spectroscopic studies of H_2 reported by He, *et al.*[18] There are three energetically accessible channels following the elimination of molecular hydrogen at 193 nm.

$H_2CCHCl \rightarrow H_2 + HCCCl$	$\Delta H_0 = 46$ kcal/mol	(rxn 7)
$H_2CCHCl \rightarrow H_2 + {}^1(:CCHCl)$	$\Delta H_0 = 91$ kcal/mol	(rxn 8)
$H_2CCHCl \rightarrow H_2 + {}^3(:CCHCl)$	$\Delta H_0 \sim 140$ kcal/mol	(rxn 9)

The majority of the observed $P(E_T)$ for H_2 elimination, shown in Figure 6, exceeds the 8 kcal/mol available energy for reaction 9, suggesting that this channel does not contribute significantly to the dissociation.

Riehl and Morokuma have calculated the recombination barrier for 1,1 elimination of H_2 to be 6 kcal/mol.[14] Such a modest recombination barrier is inconsistent with the large average translational energy release of 20 kcal/mol we observed. A small forward barrier for the isomerization of chlorovinylidene to chloroacetylene suggests a mechanism for H_2 elimination directly analogous to the concerted elimination/isomerization mechanism proposed for the HCl channel.[10]

Although *ab initio* calculations failed to locate a transition state for 1,2 elimination, the recombination barrier should be substantially higher than the corresponding barrier for reaction 8. He *et al.* concluded based on the maximum product

recoil that the major dissociation channel was 1,2 elimination.[18] The authors suggested a possible additional contribution from three center elimination involving H-atom migration to form the chloroethylidene radical intermediate, followed by 1,1 H_2 elimination. Such a mechanism would be consistent with the large observed translational energy release, as it would also result in production of H_2 and acetylene in close proximity similar to the 1,2 HCl elimination channel.

B. Atomic Elimination Channels

Atomic hydrogen elimination. Mo *et al.* have reported isotropic H atom Doppler profiles following 193 nm excitation of vinyl chloride,[6] attributing this channel to electronic predissociation, presumably involving internal conversion from the initially excited $\pi\pi^*$ state. The authors measured an average translational energy release of 17 ± 2 kcal/mol for the H atom photofragments. This large translational energy release, 35% of the available energy for H atom elimination, is inconsistent with a barrierless dissociation in the ground state. Our measured $P(E_T)$, which only includes the distribution greater than 11 kcal/mol, provides a rigorous upper limit of $\langle E_T \rangle = 18$ kcal/mol. From our measurements of the Cl photoproducts derived from secondary decomposition of chlorovinyl radicals, we have direct evidence that the total primary $P(E_T)$ must extend below the truncation point. Therefore, the average translational energy release may be significantly lower than our upper limit of 18 kcal/mol. The $P(E_T)$ for analogous H atom elimination channels in ethylene[29] and acrylonitrile[20] at 193 nm were found to be consistent with statistical partitioning of the available energy. Although we are unable to measure the complete $P(E_T)$ for H atom elimination, the majority of the evidence suggests that the complete distribution is consistent with simple bond rupture on the electronic ground state. We are unable to provide an explanation for the anomalous high average translational energy reported by Mo *et al.* The discrepancy is even more startling in light of the evidence presented below for a large additional component to the single-photon H atom signal derived from secondary dissociation of hot vinyl radicals.

Atomic chlorine elimination. Two components in the Cl translational energy distributions from the dissociation of vinyl chloride at 193 nm have been previously identified.[4,5,16] Umemoto *et al.* originally suggested that the two dissociation channels originated from primary C-Cl bond cleavage on different potential energy surfaces.[4] The low velocity channel was assigned to dissociation on the electronic ground state following internal conversion, and the high velocity channel was assigned to direct dissociation on the low lying $n\sigma^*_{(C\text{-}Cl)}$ state. The anisotropy parameters for the ground state and excited state Cl elimination channels were measured to be $\beta=0.3\pm0.2$ and $\beta=1.1\pm0.2$ respectively. A value of $\beta=1.1$ is consistent with the symmetry of the initial $\pi\pi^*$ excited state suggesting a prompt dissociation on the time scale of parent rotation. Based on *ab initio* calculations, Suzuki and co-workers have reassigned the repulsive state responsible for the translationally fast Cl elimination channel.[17] The calculated vertical excitation energy for the $n\sigma^*$ state exceeded the 193 nm photon energy suggesting that the crossing may be with the lower $\pi\sigma^*$ state. While there is no coupling between the $\pi\pi^*$ and $\pi\sigma^*_{(C\text{-}Cl)}$ states in a strictly planar geometry, the C=C twist excited following the initial $\pi^*\leftarrow\pi$ excitation relaxes the symmetry and result in an avoided crossing between the two surfaces.[37] Since the energies of the repulsive states are changing rapidly in the Franck-Condon region, we find the assignment of the dissociative state speculative in spite of the energetic arguments. We have determined that the direct Cl elimination channel accounts for 86% of Cl photofragments. This is in agreement with the 84% reported by Suzuki and co-workers[17] but is a much larger fraction than deduced from REMPI Doppler measurements.[6,9] Our measured average translational energy release, $\langle E_T\rangle=23\pm1$, agrees with previous measurements which have all assumed a Gaussian functional form for this component of the translational energy distribution.

Our measured $P(E_T)$ for the primary Cl elimination channel on the electronic ground state is shown as the solid line in the top of Figure 14. A prior distribution calculated assuming an available energy of 28 kcal/mol, half of the true available energy for reaction 10, is shown for comparison. This result suggests that there may not be

complete randomization of energy among all the vibrational modes prior to dissociation. The $P(E_T)$ previously reported for this channel by Gordon and co-workers included the contribution from faster secondary Cl atoms and therefore overestimated the translational energy release from primary Cl elimination on the ground state.[6,9]

C. Secondary Dissociation Processes

Secondary decomposition of vinyl radical intermediates and rotational metastability. There are two independent pieces of evidence for vinyl radical decomposition. The first is the lack of C_2H_3 fragments momentum matched to the slow primary C-Cl cleavage channel. The second is a contribution in the m/e 26 TOF spectra consistent with C_2H_3 dissociation. The secondary dissociation of C_2H_3 is not surprising, although it has not been considered previously. The measured $P(E_T)$ for the decomposition of vinyl radicals produced in the 193 nm photodissociation of ethylene indicated little barrier to recombination.[29] The barrier to C-H bond cleavage in the vinyl radical is just the endothermicity of 34 kcal/mol,

$$H_2CCH^{\ddagger} \rightarrow H + HCCH \qquad \Delta H_0 = 34 \text{ kcal/mol} \qquad \text{(rxn 10)}$$

Any available energy following primary C-Cl bond cleavage that is not partitioned into electronic excitation of the Cl atoms or product translation must appear as internal energy of the vinyl radicals. The available energy is 53 and 51.5 kcal/mol for Cl atoms produced in either their ground or excited spin orbit states. Given the endothermicity of 34 kcal/mol for secondary C-H bond cleavage in the vinyl radical, the minimum translational energy required for survival of vinyl radicals is 19 or 16.5 kcal/mol. We can estimate the importance of this channel based on contributions in the m/e 26 TOF spectra. The secondary dissociations of C_2H_3 and C_2H_2Cl contribute similar amounts of C_2H_2. The two components of slow Cl also are formed in similar amounts. Thus, while the primary H

yield matches the total C_2H_2Cl yield, the secondary H yield from slow vinyl radicals matches the yield of dissociative C_2H_2Cl. If most of the C_2H_2Cl undergoes secondary dissociation, up to half of the total H yield can be attributed to secondary fragmentation of vinyl radicals. The average translational energy for the secondary H-atoms in the primary center-of-mass frame is only 3-4 kcal/mole. A weighted average of the H-atoms from both primary and secondary origins should result in an average translational energy inexplicably much lower than the 17 kcal/mol reported by Mo *et al.*[6]

Given an available energy of 53 kcal/mol following C-Cl bond cleavage it is interesting to note the detection of vinyl radical photoproducts corresponding to a translational energy release of <19 kcal/mol, since these fragments have internal energy in excess of their dissociation threshold. Vinyl radicals with translational energies down 9 kcal/mol are metastable with lifetimes which are comparable to their neutral flight time of ~50 μsecs. In an investigation of the photodissociation of vinyl bromide at 193 nm, Wodtke *et al.* suggested the formation of electronically excited vinyl radical following Br elimination based on a similar observation.[38] Their measurements suggested an excited electronic state of the vinyl radical 42 kcal/mol above the electronic ground state. If vinyl radicals are produced in this excited electronic state, the available energy following primary C-Cl bond cleavage is only 11 kcal/mol. Therefore, although the production of excited C_2H_3 could account for metastable vinyl radicals corresponding to the portion of the $P(E_T)$ below 11 kcal/mol, this channel can not account for those metastable vinyl radical products formed with translational energies between 11 and 19 kcal/mol. A more likely explanation is rotational metastability. Rotational excitation of the vinyl radicals following the impulsive C-Cl bond cleavage on the excited state could be sufficient to account for the observed metastability. A particularly dramatic example of this effect has been observed by Hintsa *et al.*[32] in the dissociation of C_2H_4BrOH. In that study C_2H_4OH radicals with up to 15 kcal/mol in excess of the dissociation threshold were detected.

Secondary decomposition of chlorovinyl radical intermediates and the barrier to Cl + acetylene. In addition to the two primary C-Cl bond cleavage channels, we have

identified and measured a third reaction channel producing Cl photofragments from the secondary decomposition of chlorovinyl radicals. The presence of this channel was inferred by Suzuki and co-workers based on an increase in the $Cl(^2P_{3/2})/Cl(^2P_{1/2})$ ratio for the translationally slow Cl atoms in decreasing the excitation wavelength from 210 nm to 193 nm.[16] Structure in the $P(E_T)$ for the low velocity Cl photofragments, made possible by the high resolution of our experimental apparatus, and the observed truncation in the $P(E_T)$ for the primary H-atom elimination have provided the first direct evidence for chlorovinyl radical decomposition in the photodissociation of vinylchloride at 193 nm. As a result, we have been able to characterize the two channels that contribute to the low velocity Cl-atoms,

$$H_2CCHCl \rightarrow Cl + H_2CCH \qquad \Delta H_0 = 90 \text{ kcal/mol} \qquad \text{(rxn 11)}$$

$$H_2CCHCl \rightarrow H + C_2H_2Cl^{\ddagger} \rightarrow H + C_2H_2 + Cl \qquad \Delta H_0 = 126 \text{ kcal/mol} \qquad \text{(rxn 12)}$$

The translational energy distributions for the two channels are shown in Figure 14 and each accounts for 7% of the total Cl photofragment yield. Previous studies have not resolved this additional, and significant, contribution from secondary dissociation of the chlorovinyl radical.[4,16] The $P(E_T)$ for C-Cl bond cleavage in the chlorovinyl radical intermediates, shown as the solid line in the bottom of Figure 14, is peaked away from zero with a maximum probability of 8 kcal/mol. This is in excellent agreement with the measured truncation in the $P(E_T)$ for C_2H_2Cl photofragments, suggesting a moderate, 11 kcal/mol recombination barrier. The high-pressure limit for the rate constant for the addition of Cl to acetylene is 5×10^{-11} cm^3 s^{-1}, with a small negative temperature dependence.[39,40] This kinetic evidence is incompatible with any significant barrier, so we look for other possible interpretations.

In the dissociation of 1,2 dichloroethylenes (DCE), Sato *et al.* needed to include secondary decomposition of the chlorovinyl radicals in order to fit their TOF data.[19] The derived $P(E_T)$ for secondary C-Cl bond cleavage from that study peaked away from zero

very similar to our reported $P(E_T)$. The authors concluded that the non-statistical $P(E_T)$ was the result of a centrifugal barrier arising from significant rotational excitation in the HCCHCl intermediate following the primary C-Cl bond cleavage. In accordance with impulsive model estimates for rotational excitation the chlorovinyl radicals from 1,2 *cis* DCE dissociation showed a more pronounced effect than 1,2 *trans* DCE.[41] In our investigation of vinyl chloride, however, the primary dissociation involves the statistical elimination of a hydrogen atom. The chlorovinyl radicals from vinyl chloride photodissociation should thus have little rotational excitation and the effect of a centrifugal barrier to dissociation should be negligible. An alternative explanation is required to explain the large secondary translational energy release. In the dissociation of 1,2 *cis* and *trans* DCE the loss of either chlorine atom can only form the β-chlorovinyl radical isomer (HCCHCl). The reaction coordinate for dissociation of this isomer involves smooth evolution into free Cl and acetylene. No recombination barrier is expected for such a process, in agreement with kinetic results. In vinyl chloride dissociation, H-atom elimination can result in either the α- or β-chlorovinyl radical. *Ab initio* calculations suggest a preference for the α-chlorovinyl radical.[14] Elongation of the C-Cl bond of this isomer will lead to Cl and vinylidene at an asymptotic energy in excess of the available energy. If, however, the C-Cl bond stretch and 1,2 H-atom migration occurred in concert, the dissociation could occur from an intermediate structure with an exit barrier consistent with our results. We are thus led to interpret the metastability of the C_2H_2Cl species as evidence that most H loss leads to CH_2=CCl, which has a barrier to Cl elimination of about 35 kcal/mol, and an even higher barrier for the 1,2 H shift isomerization to HCCHCl. Figure 1b illustrates this hypothesis.

Some additional support for this interpretation can be found in the PTS data of Sato *et al.*,[19] which shows significant differences between the behavior of 1,2 DCE isomers and 1,1 DCE. Ground state elimination of atomic Cl from 1,1 DCE forms the α-chlorovinyl radical with more available energy than H elimination from vinyl chloride at 193 nm. Secondary H atom loss will be energetically accessible in the case of 1,1 DCE

but not in vinyl chloride. Cl atom loss, which we believe to be a lower energy, secondary dissociation channel from the α-chlorovinyl radical, was rejected in the analysis of Sato *et al.* based on the energetic inaccessibility of Cl + :CCH_2. Only in the case of 1,1 DCE does the reported $P(E_T)$ for the Cl atoms include extra partially resolved, and unassigned structure.[13] We believe a more comprehensive interpretation of the 1,1 DCE PTS data of Sato *et al.* could be achieved with the inclusion of a secondary Cl loss from the $ClCCH_2$ radical, using the exit barrier we propose in this work.

5. Conclusion

Using the technique of PTS with tunable VUV undulator radiation we have investigated the dissociation of vinyl chloride following $\pi^* \leftarrow \pi$ excitation at 193 nm. We have identified one dissociation channel which occurs following crossing to a directly dissociative PES ($\pi\sigma^*_{(C\text{-}Cl)}$) resulting in Cl elimination with a large translational energy release. We have identified four primary dissociation channels that occur on the ground PES following internal conversion from the initially excited $\pi\pi^*$ PES including HCl elimination, H atom elimination, Cl elimination, and H_2 elimination. In addition, we have directly measured secondary decomposition of primary chlorovinyl radical and vinyl radical photoproducts. We have measured c.m. translational energy distributions for all of the dissociation channels. From the truncation of the $P(E_T)$ for surviving chlorovinyl radical photoproducts we have made a direct measurement of the recombination barrier for Cl + acetylene of 11±2 kcal/mol. We interpret this recombination barrier to be on a concerted path to the α-chlorovinyl radical, since the β-chlorovinyl radical is not expected to have any significant barrier to Cl loss in excess of the endothermicity. We have measured the photoionization spectrum for HCl photoproducts providing a qualitative indication that ~40% of the available energy for the HCl elimination channel is partitioned into internal degrees of freedom in the HCl photofragments, in agreement with previous work.

Acknowledgments

This work was supported by the Director, Office of Energy Research, Office of Basic Energy Science, Chemical Sciences Division of the U. S. Department of Energy under contract No. DE-AC03-76SF00098. The experiments were conducted at the Advanced Light Source, Lawrence Berkeley National Laboratory which is supported by the same source. Work by SWN and GEH at Brookhaven National Laboratory was performed under contract No. DE-AC02-76CH00016 with the U.S. Department of Energy and supported by its Chemical Sciences Division.

References

[1] M. J. Berry, *J. Chem. Phys.* **61**, 3114, (1974); M. J. Molina and G. C. Pimentel, *J. Chem. Phys.* **56**, 3988 (1972).

[2] M. G. Moss, M. D. Ensminger, and J. D. McDonald, *J. Chem. Phys.* **74**, 6631 (1981).

[3] D. J. Donaldson and S. R. Leone, *Chem. Phys. Lett.* **132**, 240 (1986).

[4] M. Umemoto, K. Seki, H. Shinohara, U. Nagashima, N. Nishi, M. Kinoshita, and R. Shimada, *J. Chem. Phys.* **83**, 1857 (1985).

[5] P. T. A. Reilly, Y. Xie, and R. J. Gordon, *Chem. Phys. Lett.* **178**, 511 (1991).

[6] Y. Mo, K. Tonokura, Y. Matsumi, M. Kawasaki, T. Sato, T. Arikawa, P. T. A Reilly, Y. Xie, Y. Yang, Y. Huang, and R. J. Gordon, *J. Chem. Phys.* **97**, 4815 (1992).

[7] G. He, Y. Yang, Y. Huang, and R. J. Gordon, *J. Phys. Chem.* **97**, 2186 (1993).

[8] Y. Huang, Y. Yang, G. He, and R. J. Gordon, *J. Chem. Phys.* **99**, 2752 (1993).

[9] Y. Huang, G. He, Y. Yang, S. Hashimoto, R. J. Gordon, *Chem. Phys. Lett.* **229**, 621 (1994).

[10] Y. Huang, Y. Yang, G. He, S. Hashimoto, R. J. Gordon, *J. Chem. Phys.* **103**, 5476 (1995).

[11] K. Sato, Y. Shihira, S. Tsunashima, H. Umemoto, T. Takayanagi, K. Furukawa, and S. Ohno, *J. Chem. Phys.* **99**, 1703 (1993).

[12] C. Reiser, F. M. Lussier, C.C. Jensen, and J. I. Steinfeld, *J. Am. Chem. Soc.* **101**, 350 (1979).

[13] K. Sato, S. Tsunashima, T. Takayanagi, K. Yokoyama, G. Fujisawa, and A. Yokoyama, *Chem. Phys. Lett.* **232** 357 (1995).

[14] J. Riehl and K. Morokuma, *J. Chem. Phys.* **100**, 8976 (1994).

[15] J. Riehl, D. G. Musaev, and K. Morokuma, *J. Chem. Phys.* **101**, 5942 (1994).

[16] T. Suzuki, K. Tonokura, L. S. Bontuyan, and N. Hashimoto, *J. Phys. Chem.* **98**, 13447 (1994).

[17] K. Tonokura, L. B. Daniels, T. Suzuki, and K. Yamashita, *J. Phys. Chem. A.* **101**, 7754 (1997).

[18] G. He, Y. Yang, Y. Huang, S. Hasimoto, and R. J. Gordon, *J. Chem. Phys.* **103**, 5488 (1995).

[19] K. Sato, S. Tsunashima, T. Takayanagi, G. Fujisawa, and A. Yokoyama, *J. Chem. Phys.* **106**, 10123 (1997).

[20] D. A. Blank, A. G. Suits, Y. T. Lee, S. W. North, and G. E. Hall, *J. Chem. Phys.*, in press.

[21] X. Yang, D. A. Blank, J. Lin, P. A. Heimann, A. M. Wodtke, A. Suits, and Y. T. Lee, *Rev. Sci. Instrum* **68**, 3317 (1997).

[22] D. A. Blank, Ph.D. Thesis, University of California, Berkeley (1997).

[23] M. Koike, P. A. Heimann, A. H. Kung, T. Namioka, R. DiGennaro, B. Gee, N. Yu, *Nuclear Instruments and Methods in Physics Research* **347**, 282 (1994); P. A. Heimann, M. Koike, C. W. Hsu, M. Evans, C. Y. Ng, D. Blank, X. M. Yang, C. Flaim, A. G. Suits, Y. T. Lee, SPIE Proceedings 2865 (1996).

[24] A. M. Wodtke, Ph.D. Thesis, University of California, Berkeley (1986); X. Zhao, Ph.D. Thesis, University of California, Berkeley (1989).

[25] X. Zhao, G. M. Nathanson, and Y. T. Lee, *Acta Physico-Chim. Sinica* **8**, 70 (1992).

[26] At room temperature the vinyl chloride reactant will contain 1-2 kcal/mol of internal energy on average and will experience substantial cooling of the internal degrees of freedom following supersonic expansion.

[27] The heats of formation for vinyl chloride, acetylene, vinyl radical, H, H_2, HCl, and Cl were taken from reference 28. The dissociation energies for H + C_2H_2Cl, H_2 + HCCCl

and H_2 + HClCC were taken from estimates in reference 14. The isomerization energy for acetylene/vinylidene and the singlet/triplet splitting for vinylidene were taken from reference 35. The singlet/triplet splitting for chlorovinyldene was assumed to be the same as the singlet/triplet splitting in vinylidene.

[28] Handbook of Chemistry and Physics, D. R. Lide (CRC, Boca Raton, 1995).

[29] B. A. Balko, J. Zhang, and Y. T. Lee, *J. Chem. Phys.* **97**, 935 (1992).

[30] S. W. North, D. A. Blank, J. D. Gezelter, C. A. Longfellow, and Y. T. Lee, *J. Chem. Phys.* **102**, 4447 (1995).

[31] S. W. North, D. A. Blank, and Y. T. Lee, *Chem. Phys. Lett.* **224**, 38 (1994); P. M. Kroger and S. J. Riley, *J. Chem. Phys.* **67**, 4483 (1977).

[32] E. J. Hinsta, X. Zhao, and Y. T. Lee, *J. Chem. Phys.* **92**, 2280 (1990).

[33] J. Berkowitz, C. A. Mayhew, and R. Ruscic, *J. Chem. Phys.* **88**, 7396 (1988).

[34] D. A. Blank, S. W. North, D. Stranges, A. G. Suits, and Y. T. Lee, *J. Chem. Phys.* **106**, 539 (1997).

[35] K. M. Ervin, J. Ho, and W. C. Lineberger, *J. Chem. Phys.* **91**, 5974 (1989).

[36] T. Carrington, L. M. Hubbard, H. F. Schaefer III, and W. H. Miller, *J. Chem. Phys.* **80**, 4347 (1984); M. M. Gallo, T. P. Hamilton, and H. F. Schaefer III, *J. Am. Chem. Soc.* **112**, 8714 (1990).

[37] T. L. Myers, D. C. Kitchen, B. Hu, and L. J. Butler, *J. Chem. Phys.* **104**, 5446 (1996).

[38] A. M. Wodtke, E. J. Hintsa, J. Somorjai, and Y. T. Lee, *Israel Journal of Chemistry*, **29**, 383 (1989).

[39] J. Brunning and L. J. Stief, *J. Chem. Phys.* **83**, 1005 (1985).

[40] W. B. DeMore, S. P. Sander, D. M. Golden, M. J. Molina, R. F. Hampson, M. J. Kurylo, C. J. Howard, A. R. Ravishankara, *Chemical kinetics and photochemical data for use in stratospheric modeling*, Evaluation number 9, JPL Publicaiton 90-1, Pasadena, CA, 1990.

[41] Using ground state equilibrium geometries and rigid fragment partitioning of the available energy.

Figure Captions

Figure 1: Thermodynamically available dissociation channels for vinyl chloride following absorption at 193 nm. A: Molecular channels, B: radical channels. Reference 27 summarizes the sources for thermodynamic values. Barriers connecting $ClCCH_2$ with ClHCCH and with Cl+HCCH illustrate hypotheses consistent with present results.

Figure 2: TOF spectrum for m/e 61 ($C_2H_2Cl^+$) photoproducts at a scattering angle of 7° and a photoionization energy of 11.0 eV. The forward convolution fits are from the $P(E_T)$ in figure 3.

Figure 3: $P(E_T)$ used to fit the TOF spectra in figure 2. The dotted lines represent the uncertainty in the point of truncation.

Figure 4: A schematic representation of the relationship between the truncation in the $P(E_T)$ for surviving chlorovinyl radical intermediates and the recombination barrier for Cl + HCCH.

Figure 5: TOF spectra for m/e 60 (C_2HCl^+) photoproducts at scattering angles of 10° and 15° and a photoionization energy of 12.0 eV. The dominant component in the forward convolution fits is from H_2 elimination, $H_2CCHCl \rightarrow H_2 + HCCCl$, and was fitted with the $P(E_T)$ shown in figure 6. The minor component in the 10° spectrum is from dissociative ionization of C_2H_2Cl photoproducts and was fitted with the $P(E_T)$ shown in figure 3.

Figure 6: $P(E_T)$ for H_2 elimination, $H_2CCHCl \rightarrow H_2 + HCCCl$, used to fit the TOF spectra shown in figure 5.

Figure 7: TOF spectra for m/e 36 (HCl^+) at scattering angles of 20° and 40° and a photoionization energy of 14.0 eV. The forward convolution fits to the TOF spectra were done with the $P(E_T)$ shown in figure 9.

Figure 8: $P(E_T)$ for HCl elimination, $H_2CCHCl \rightarrow HCl + C_2H_2$, used to fit the TOF spectra shown in figure 8.

Figure 9: Integrated signal intensity for m/e 36 (HCl^+) photoproduct at a scattering angle of 20° plotted as a function of the undulator photoionization energy.

Figure 10: TOF spectra for m/e 27 ($C_2H_3^+$) photoproducts at scattering angles of 15° and 25° and a photoionization energy of 11.0 eV. The forward convolution fits to the spectra were done using the $P(E_T)$ in figure 11.

Figure 11: $P(E_T)$ for C-Cl bond cleavage, $H_2CCHCl \rightarrow Cl + C_2H_3$, on the excited electronic state used in the forward convolution fits for the TOF in figures 10, 12, and 15.

Figure 12: TOF spectrum for m/e 35 (Cl^+) photoproducts at a scattering angle of 7° and a photoionization energy of 14.0 eV. The forward convolution fit to the spectra used the $P(E_T)$ in figure 11 for the fast component and figure 13 for the slow component.

Figure 13: Translational energy distribution for the slow Cl photoproducts. The forward convolution fit to the TOF data in figure 12 is the dashed line

representing the component from ~60-200 μsecs. Note that this is the translational energy distribution for Cl fragments alone and not the *total* c.m. translational energy distribution.

Figure 14: Translational energy distributions for the two product channels that make up the slow Cl photofragments for which the $P(E_T)$ is shown in figure 13. **TOP:** $P(E_T)$ for C-Cl bond cleavage, $H_2CCHCl \rightarrow Cl + C_2H_3$, on the ground PES, solid line. Prior distribution calculated given 25 kcal/mol of available energy, dashed line. **BOTTOM:** $P(E_T)$ for primary chlorovinyl radical intermediates that undergo secondary decomposition, $H_2CCHCl \rightarrow H + C_2H_2Cl^{\ddagger}$, dashed line. $P(E_T)$ for secondary decomposition of chlorovinyl radical intermediates, $C_2H_2Cl^{\ddagger} \rightarrow Cl + HCCH$, solid line.

Figure 15: TOF spectra for m/e 35 ($^{35}Cl^+$) photoproducts at scattering angles of 7°, 15°, and 25°, and a photoionization energy of 14.0 eV. The sharp component at early arrival times, dashed line, was fitted with the $P(E_T)$ in figure 12 for C-Cl bond cleavage on the $\pi\sigma^*_{(C\text{-}Cl)}$ PES. The products at later arrival times, dashed line, were fitted with the $P(E_T)$ in figure 13. The slower component was then broken into two components, dotted lines, involving C-Cl bond on the ground PES, $P(E_T)$ shown in top of figure14, and secondary decomposition of primary chlorovinyl radical intermediates, $P(E_T)$s shown in bottom of figure 14.

Figure 16: The dependence of the integrated signal at m/e 27 ($C_2H_3^+$) and scattering angle of 20° on the undulator photoionization energy.

Figure 17: TOF spectra for m/e 26 ($C_2H_2^+$) at a scattering angle of 10° and a photoionization energy of 11.0 eV and scattering angles of 10° and 20° and

a photoionization energy of 14.0 eV. The contributions to the forward convolution fits are from the following dissociation channels: **(a)** $H_2CCHCl \rightarrow HCl + HCCH$, **(b)** $H_2CCHCl \rightarrow H + H_2CCCl^{\ddagger} \rightarrow H + Cl + HCCH$, **(c)** $H_2CCHCl \rightarrow Cl + H_2CCH^{\ddagger} \rightarrow Cl + H + HCCH$, **(d)** $H_2CCHCl \rightarrow Cl + H_2CCH$ (dissociatively photoionized). A complete discussion of the contributions to the m/e 26 TOF spectra is presented in the text.

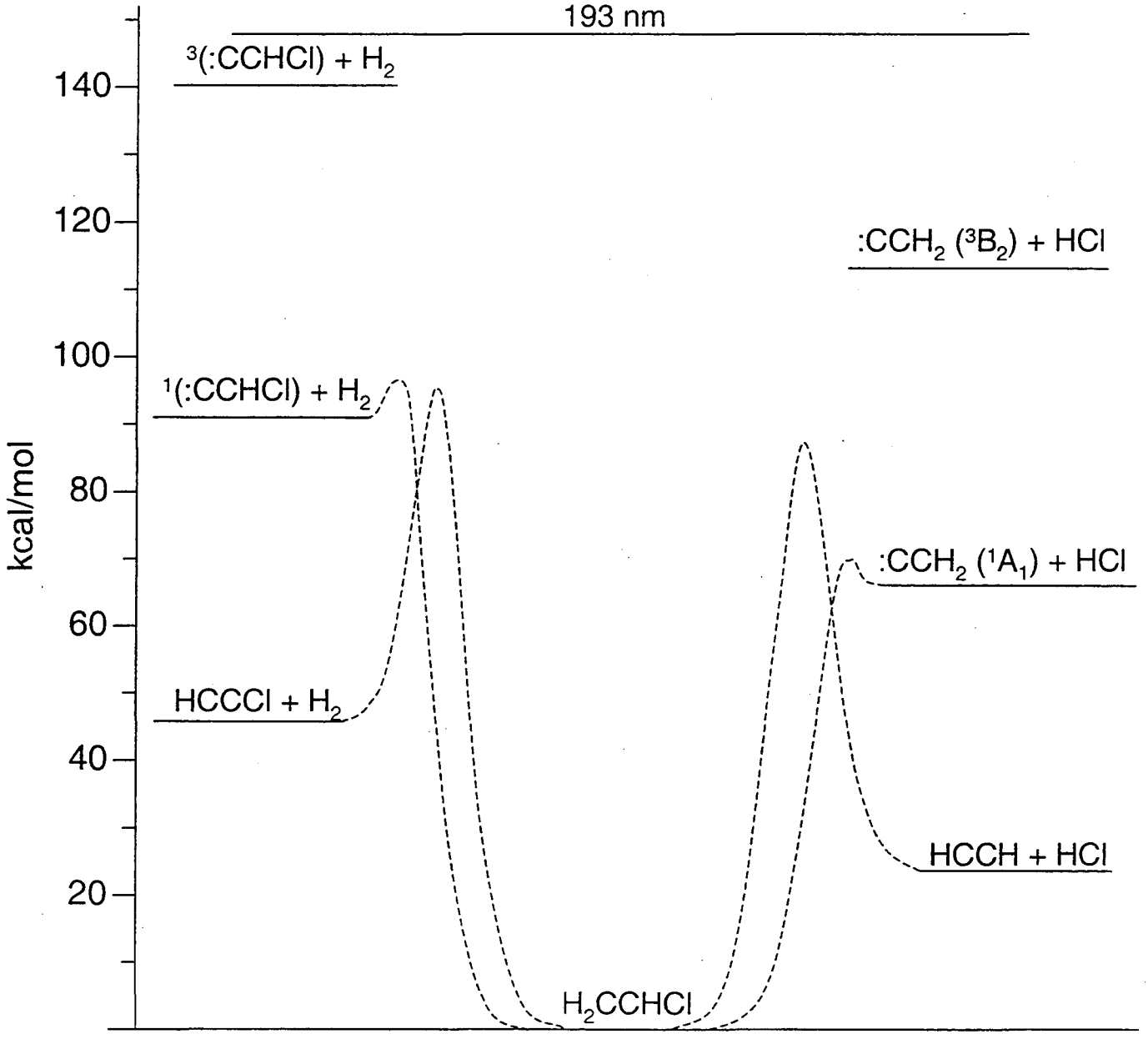
193 nm
^{3}(:CCHCl) + H_2
140
120
100
80
60
40
20
kcal/mol
:CCH_2 ($^3B_2$) + HCl
^{1}(:CCHCl) + H_2
:CCH_2 ($^1A_1$) + HCl
HCCCl + H_2
HCCH + HCl
H_2CCHCl

figure 1a

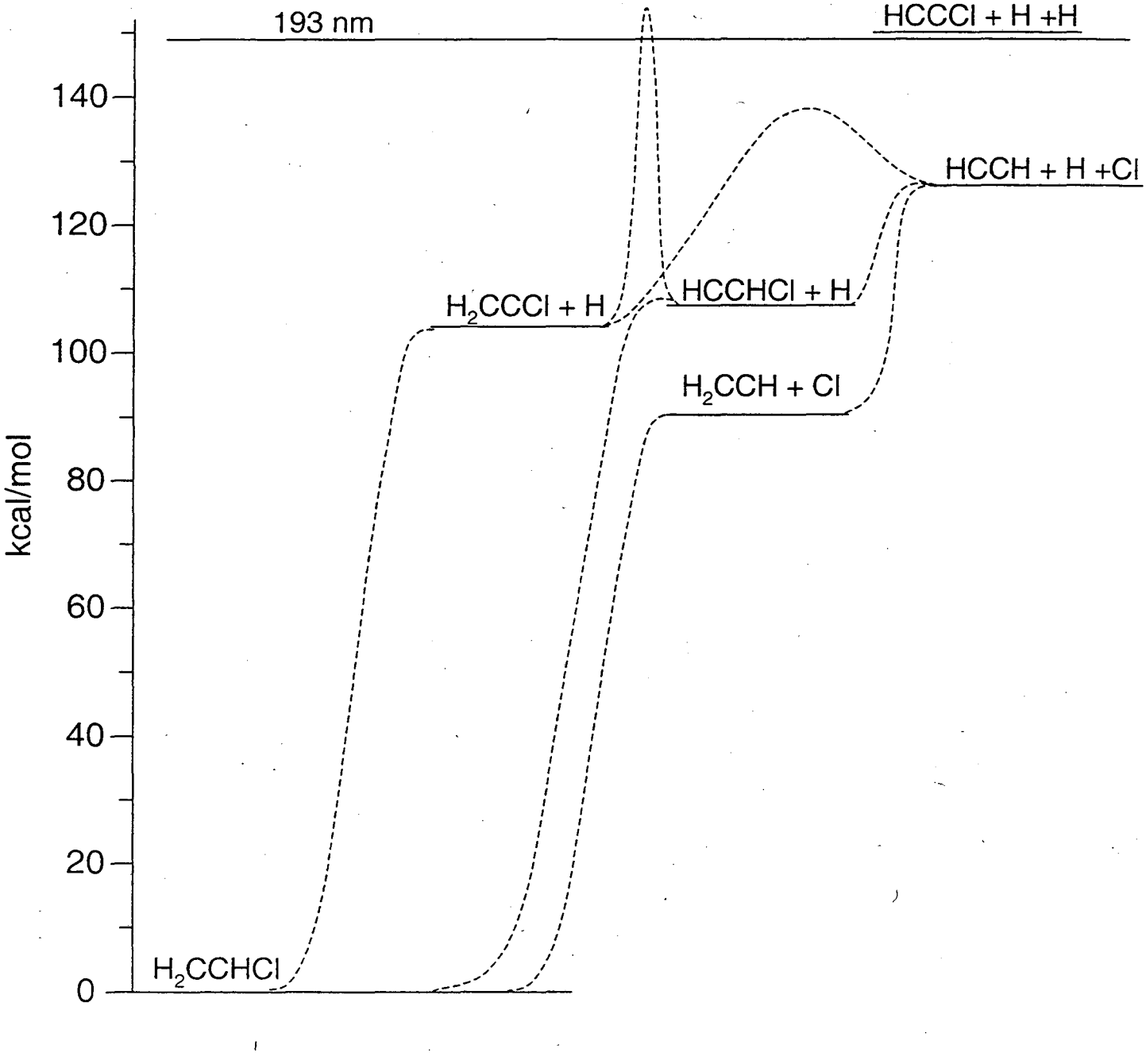
193 nm
HCCCl + H +H
HCCH + H +Cl
HCCHCl + H
H2CCCl + H
H2CCH + Cl
H2CCHCl
kcal/mol
140
120
100
80
60
40
20
0

figure 1b

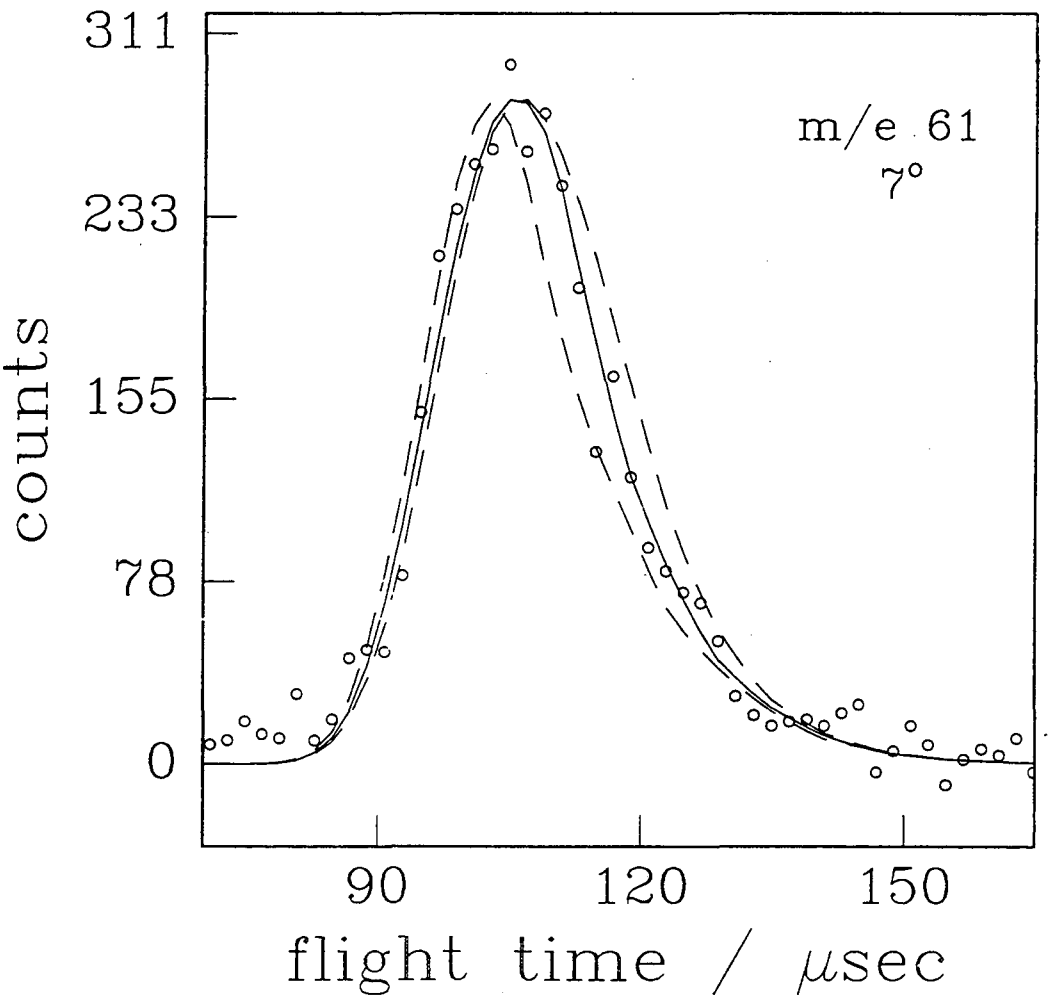

figure 2

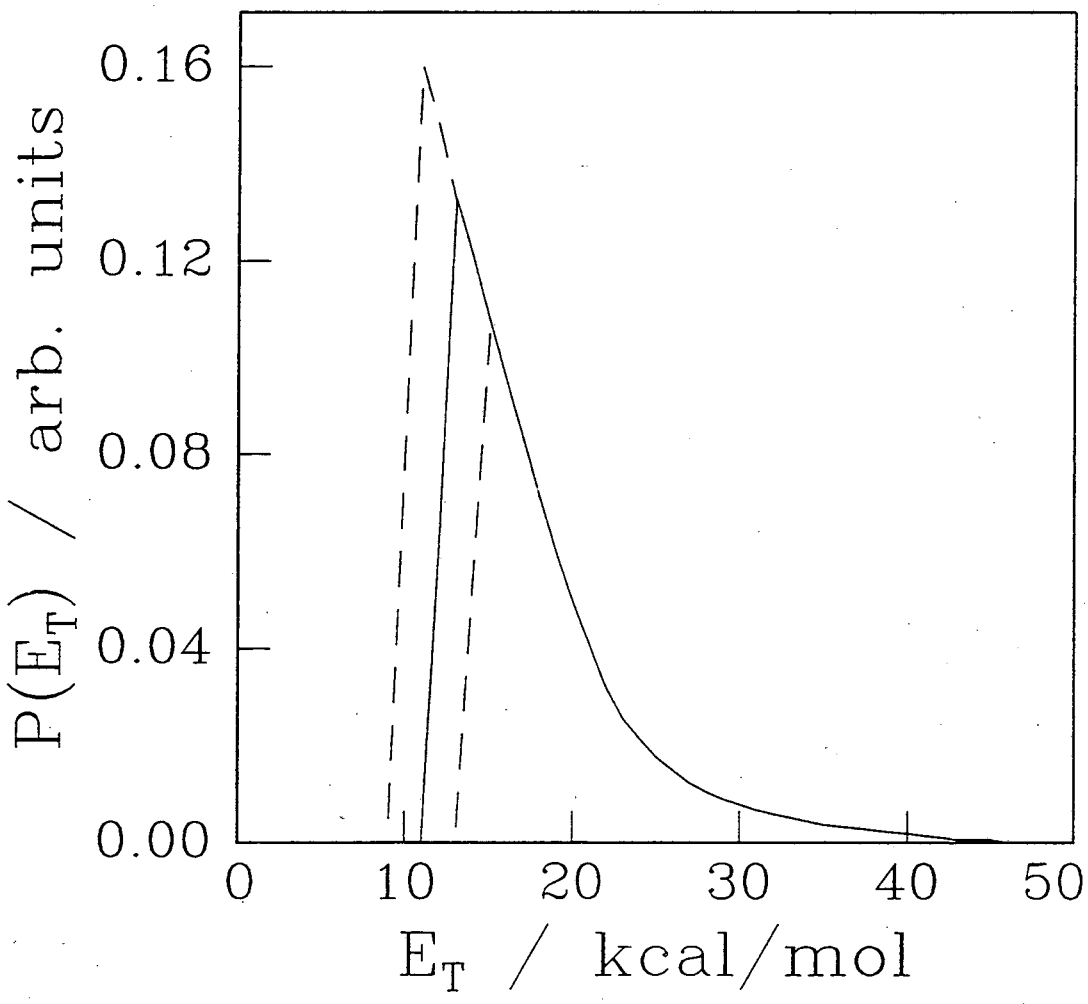

figure 3

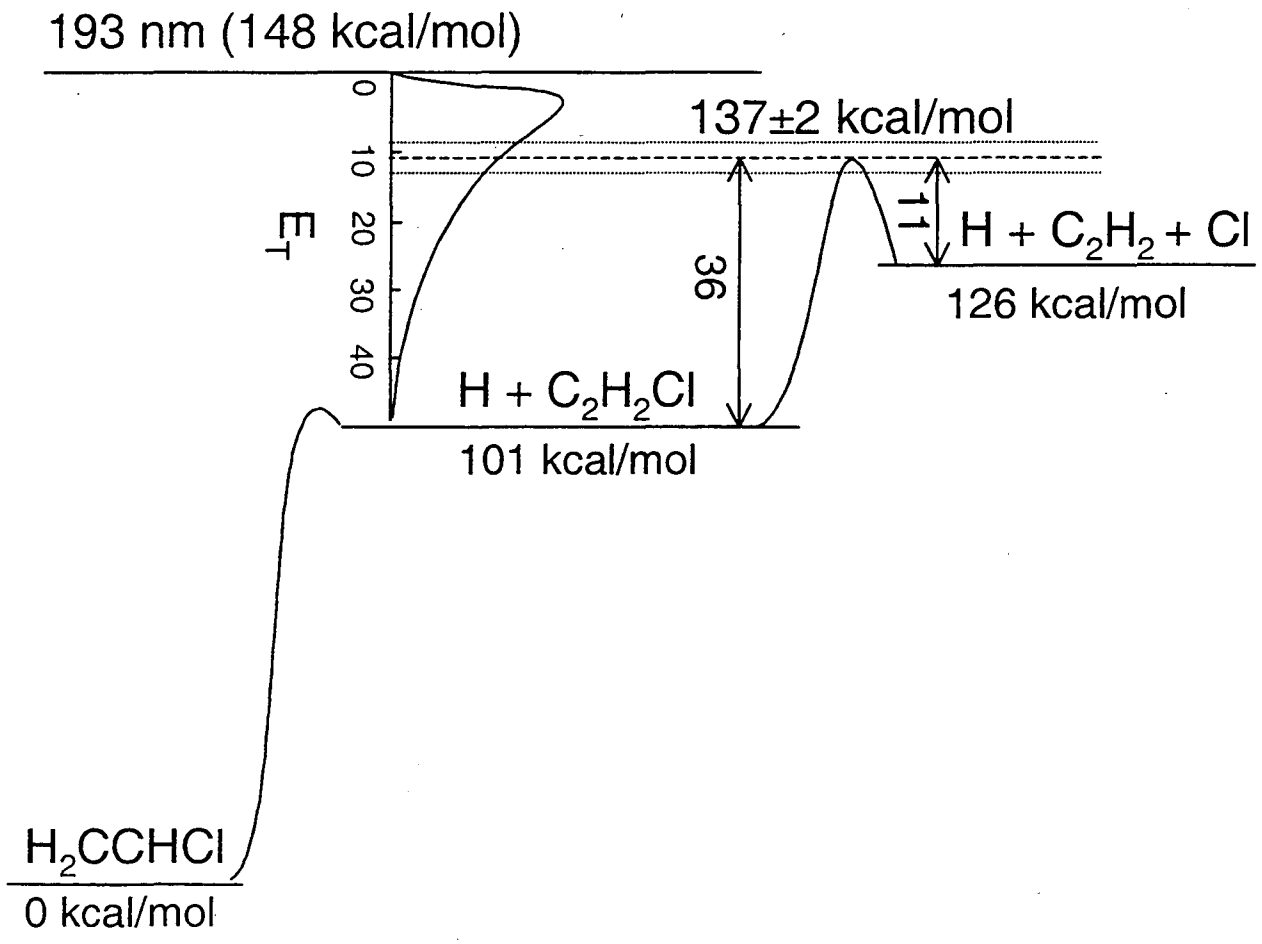
193 nm (148 kcal/mol)
0
10
20
30
40
E_T
137±2 kcal/mol
36
11
$H + C_2H_2 + Cl$
126 kcal/mol
$H + C_2H_2Cl$
101 kcal/mol
H_2CCHCl
0 kcal/mol

figure 4

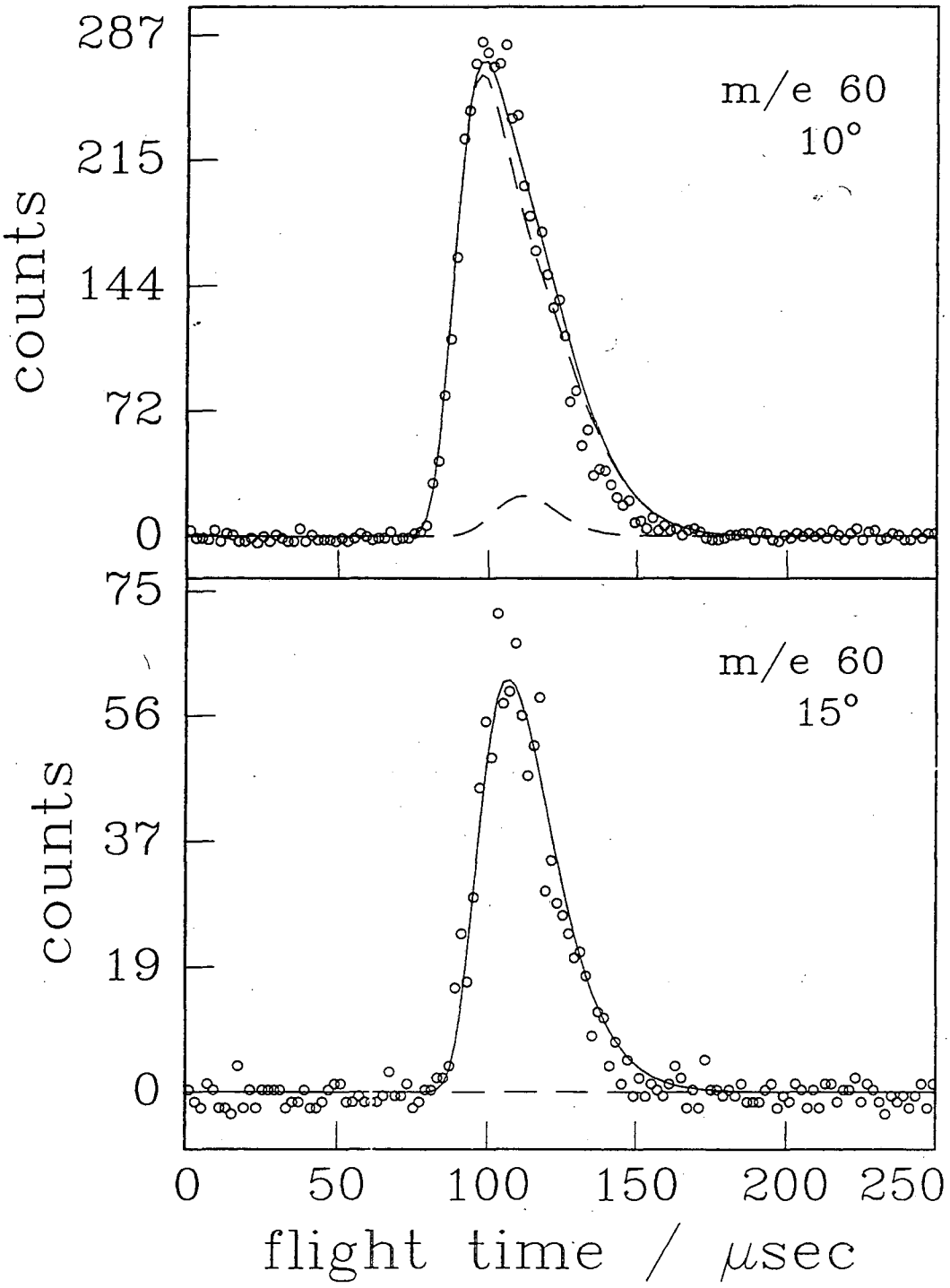
287
215
144
72
0
counts
m/e 60
10°
75
56
37
19
0
counts
m/e 60
15°
0
50
100
150
200
250
flight time / μsec

figure 5

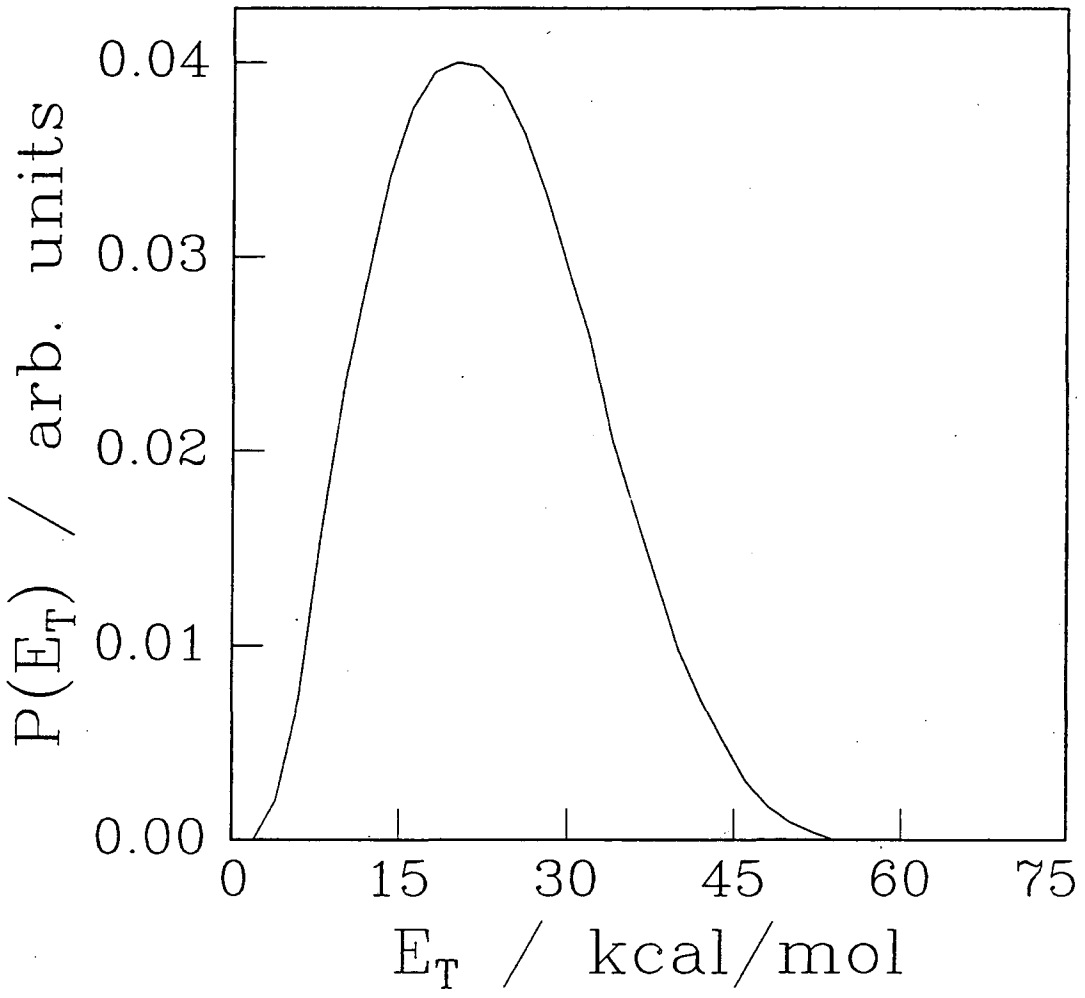

figure 6

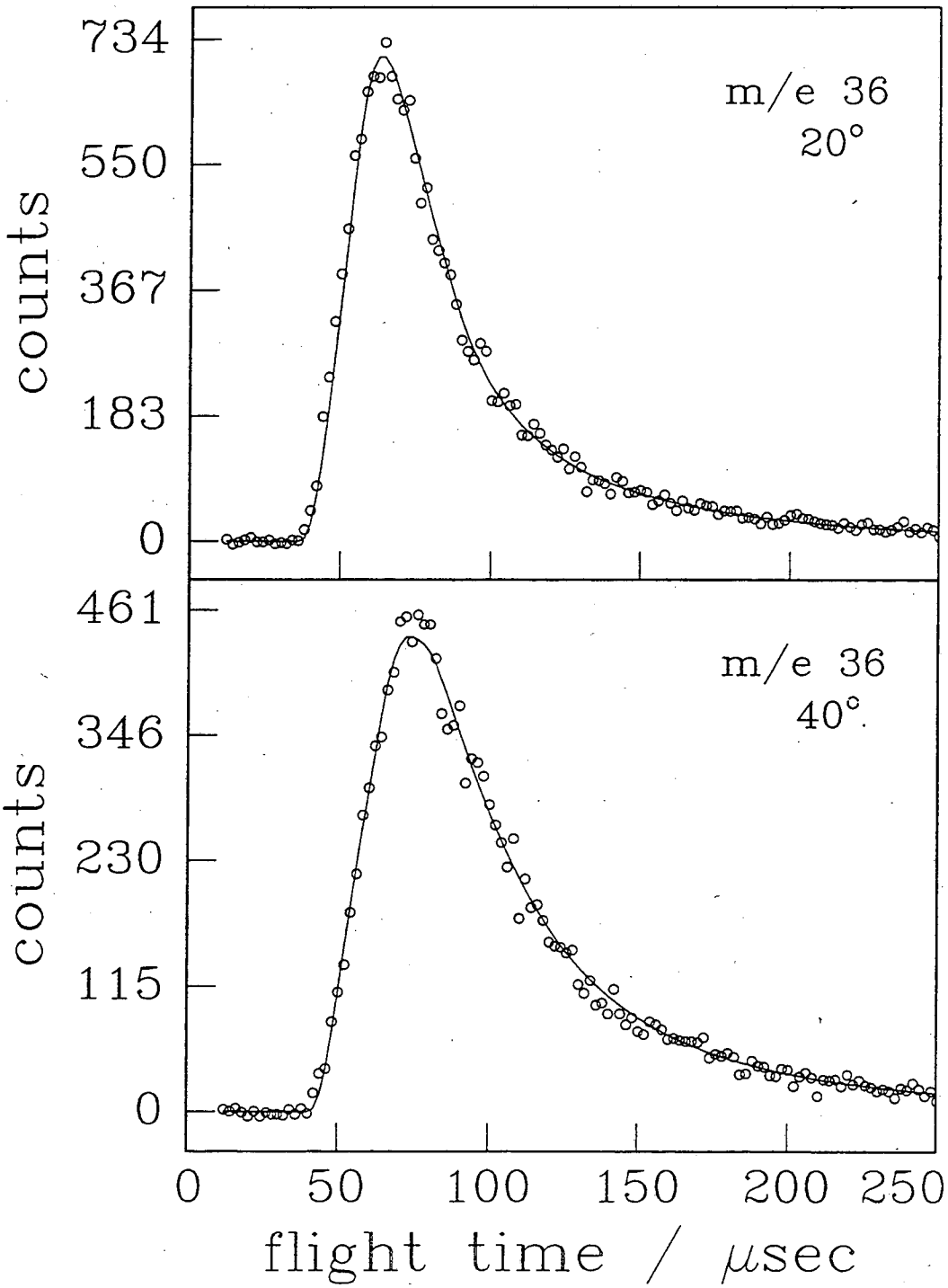
734
550
367
183
0
counts
m/e 36
20°
461
346
230
115
0
counts
m/e 36
40°
0
50
100
150
200
250
flight time / μsec

figure 7

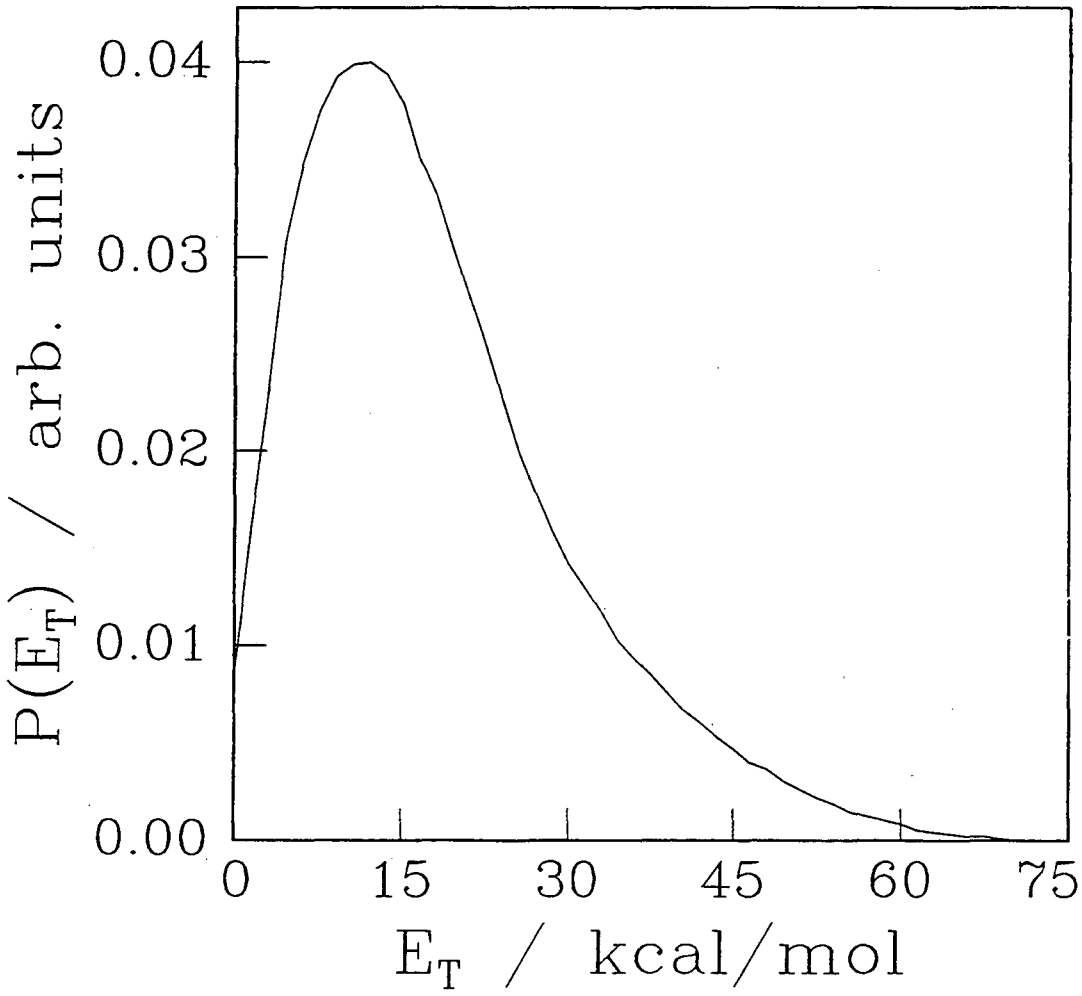

figure 8

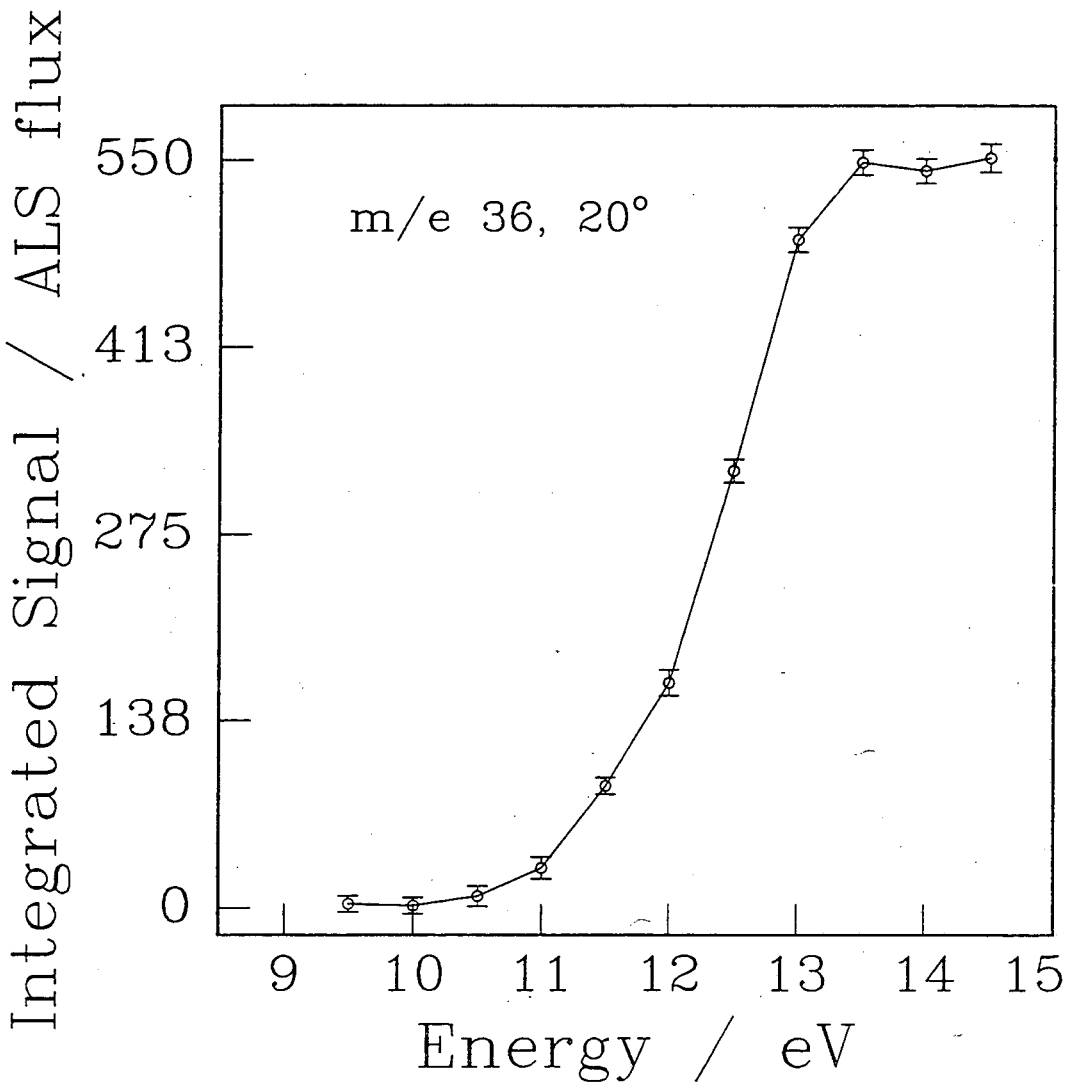
Integrated Signal / ALS flux
550
413
275
138
0
m/e 36, 20°
9
10
11
12
13
14
15
Energy / eV

figure 9

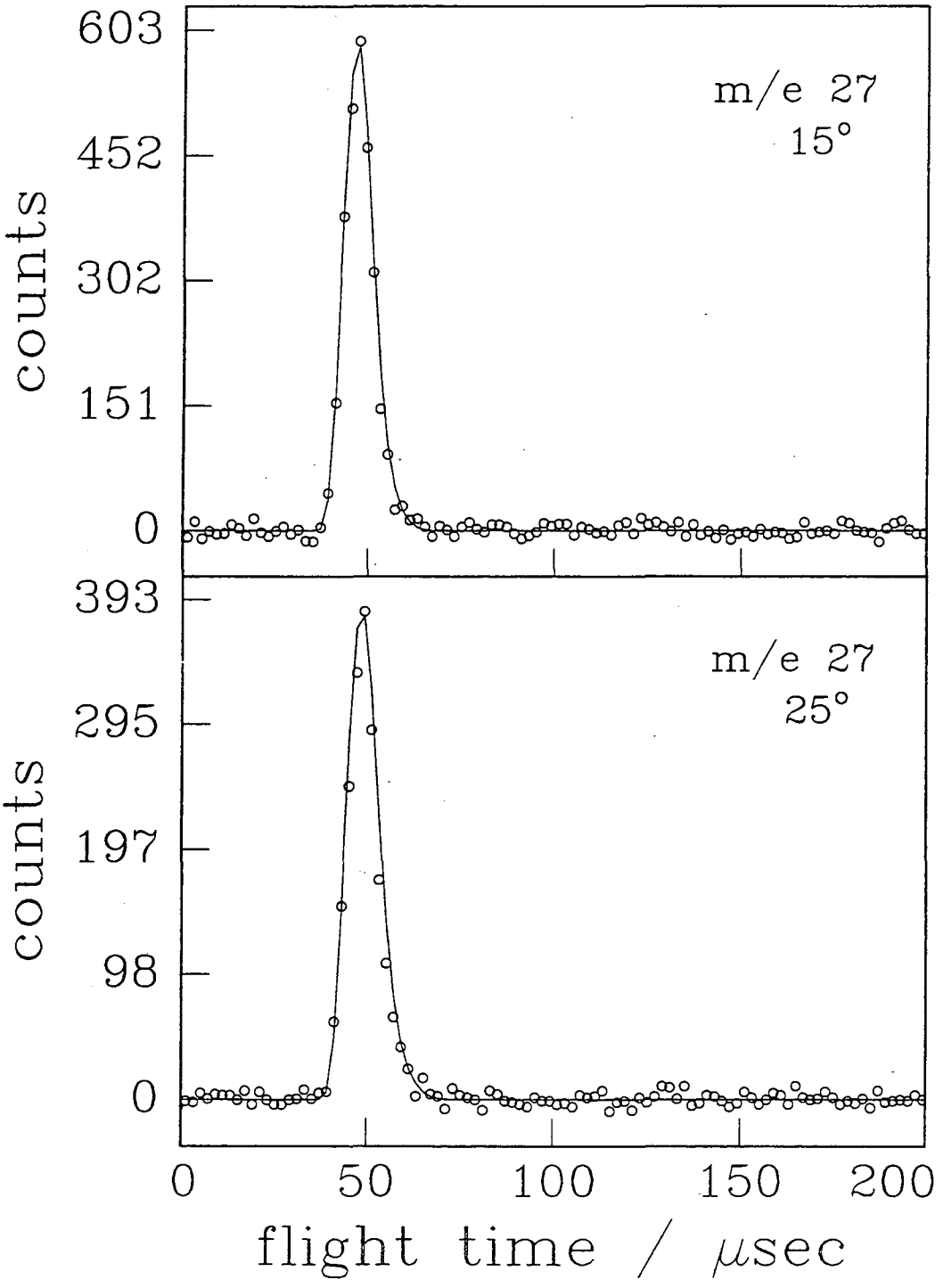
603
452
302
151
0
counts
m/e 27
15°
393
295
197
98
0
counts
m/e 27
25°
0
50
100
150
200
flight time / μsec

figure 10

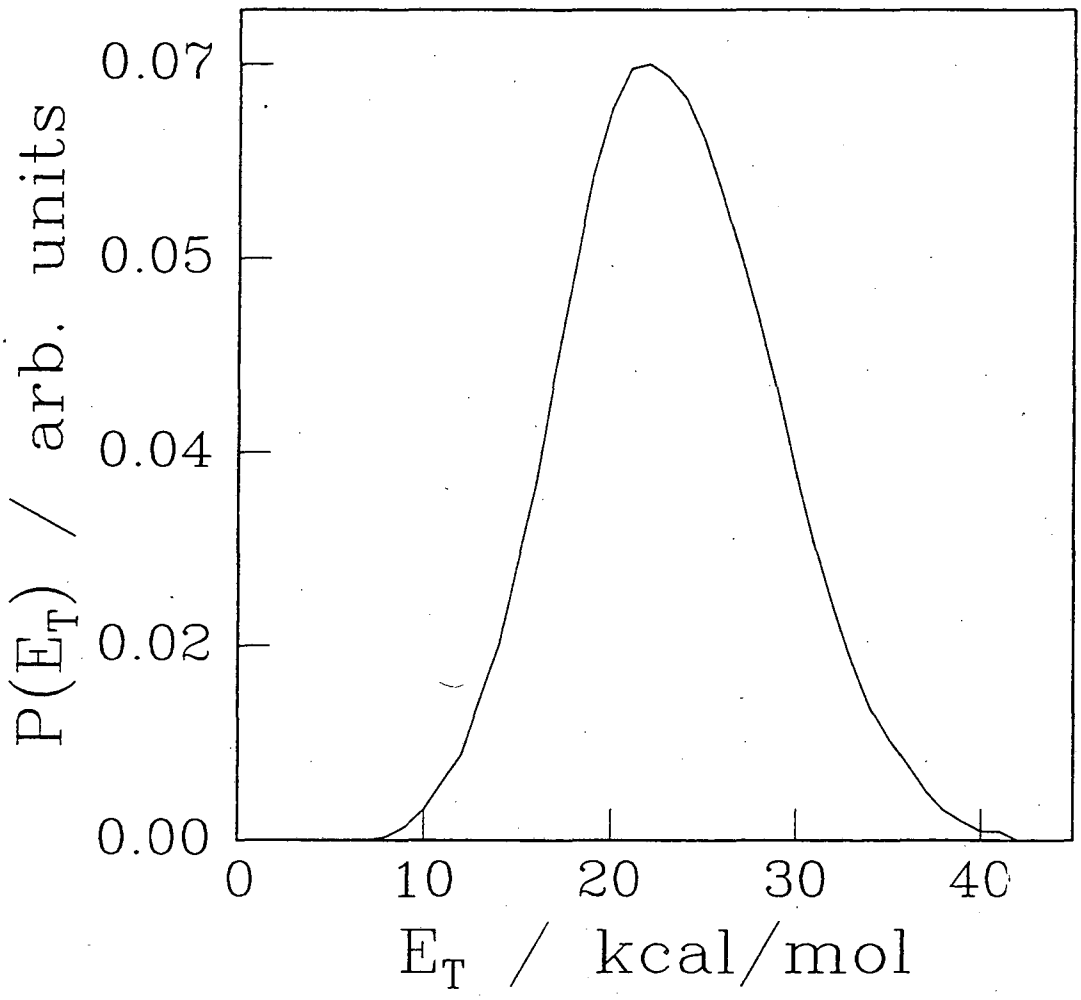

figure 11

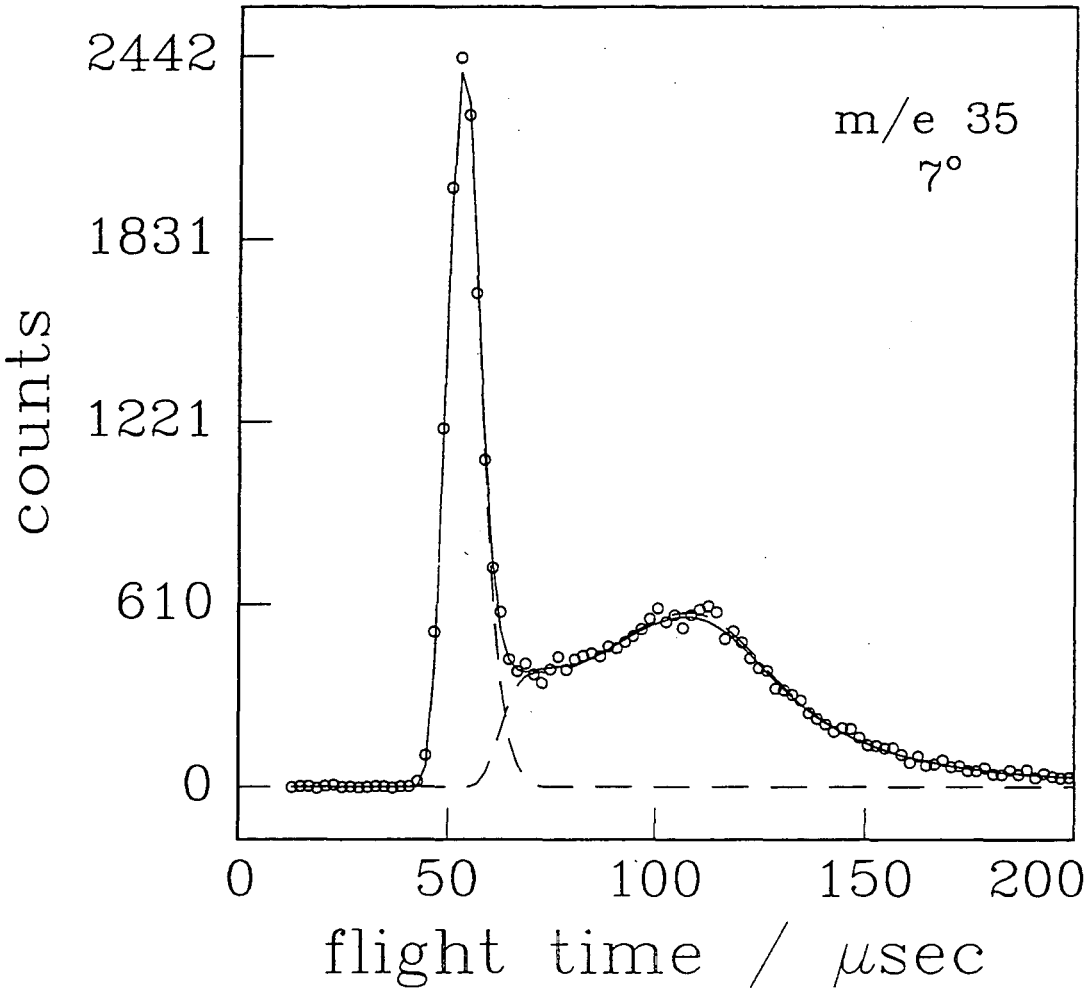
2442
1831
1221
610
0
counts
m/e 35
7°
0
50
100
150
200
flight time / μsec

figure 12

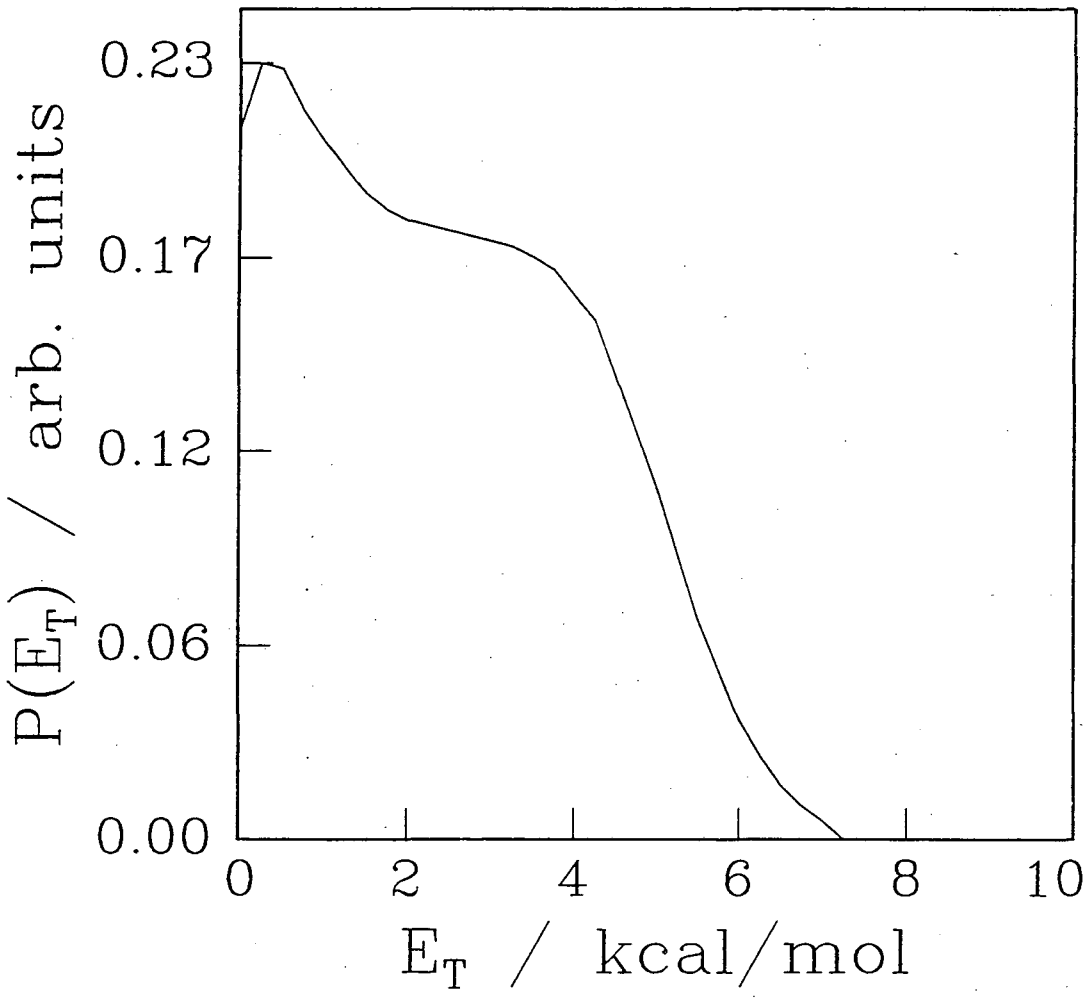

figure 13

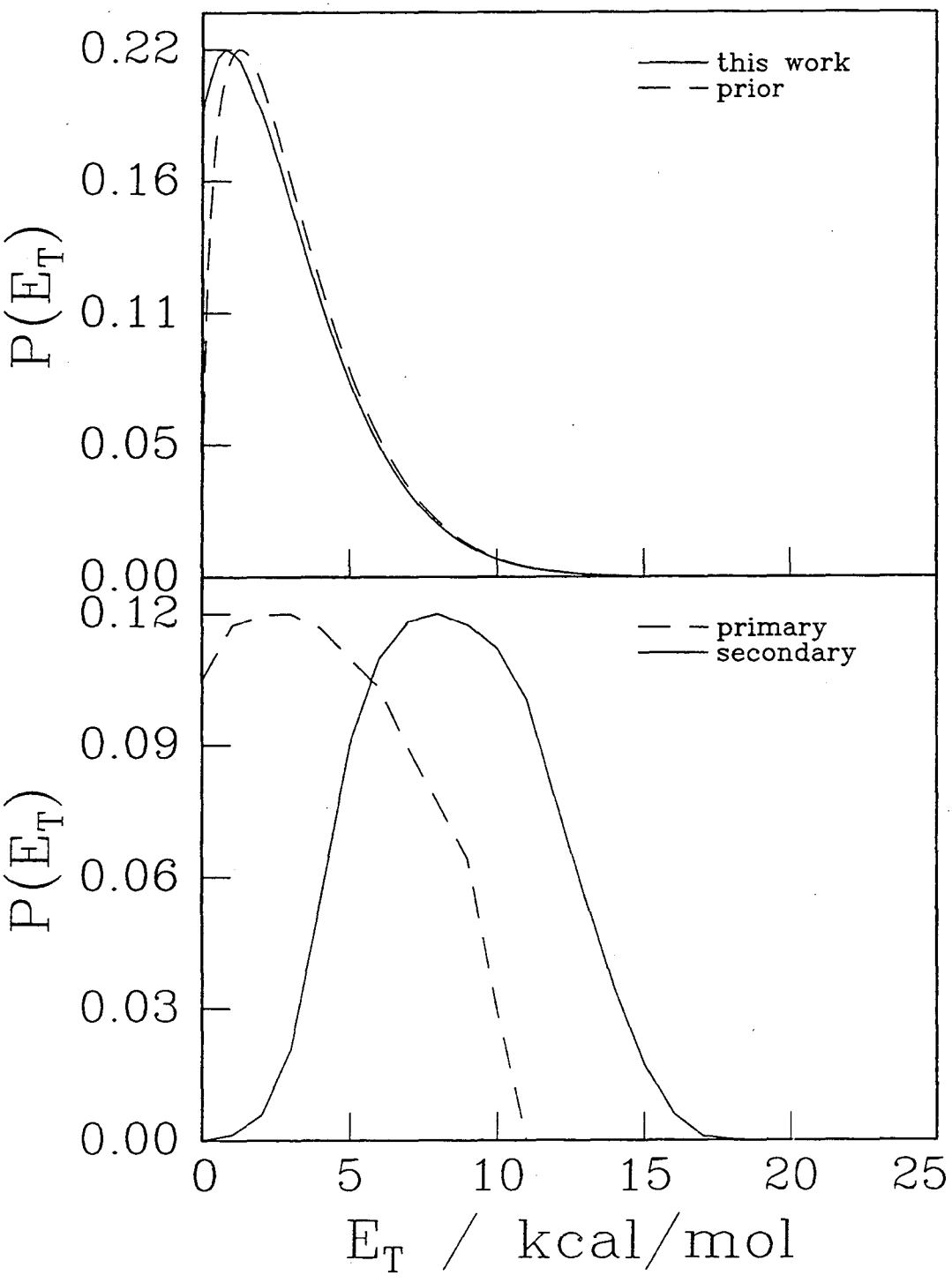
0.22
0.16
0.11
0.05
0.00
P(E_T)
this work
prior
0.12
0.09
0.06
0.03
0.00
P(E_T)
primary
secondary
0
5
10
15
20
25
E_T / kcal/mol

figure 14

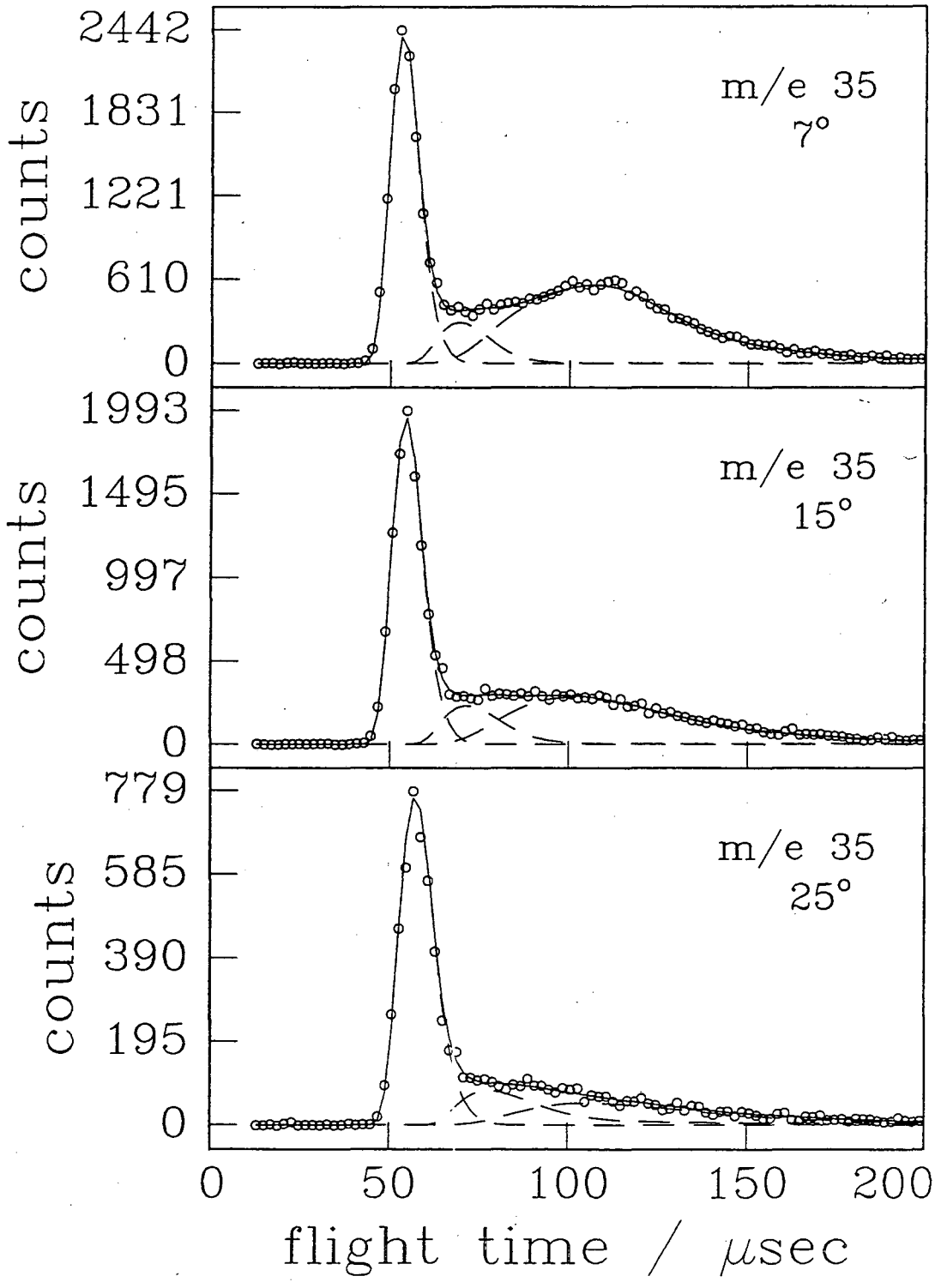
2442
1831
1221
610
0
counts
m/e 35
7°
1993
1495
997
498
0
counts
m/e 35
15°
779
585
390
195
0
counts
m/e 35
25°
0
50
100
150
200
flight time / μsec

figure 15

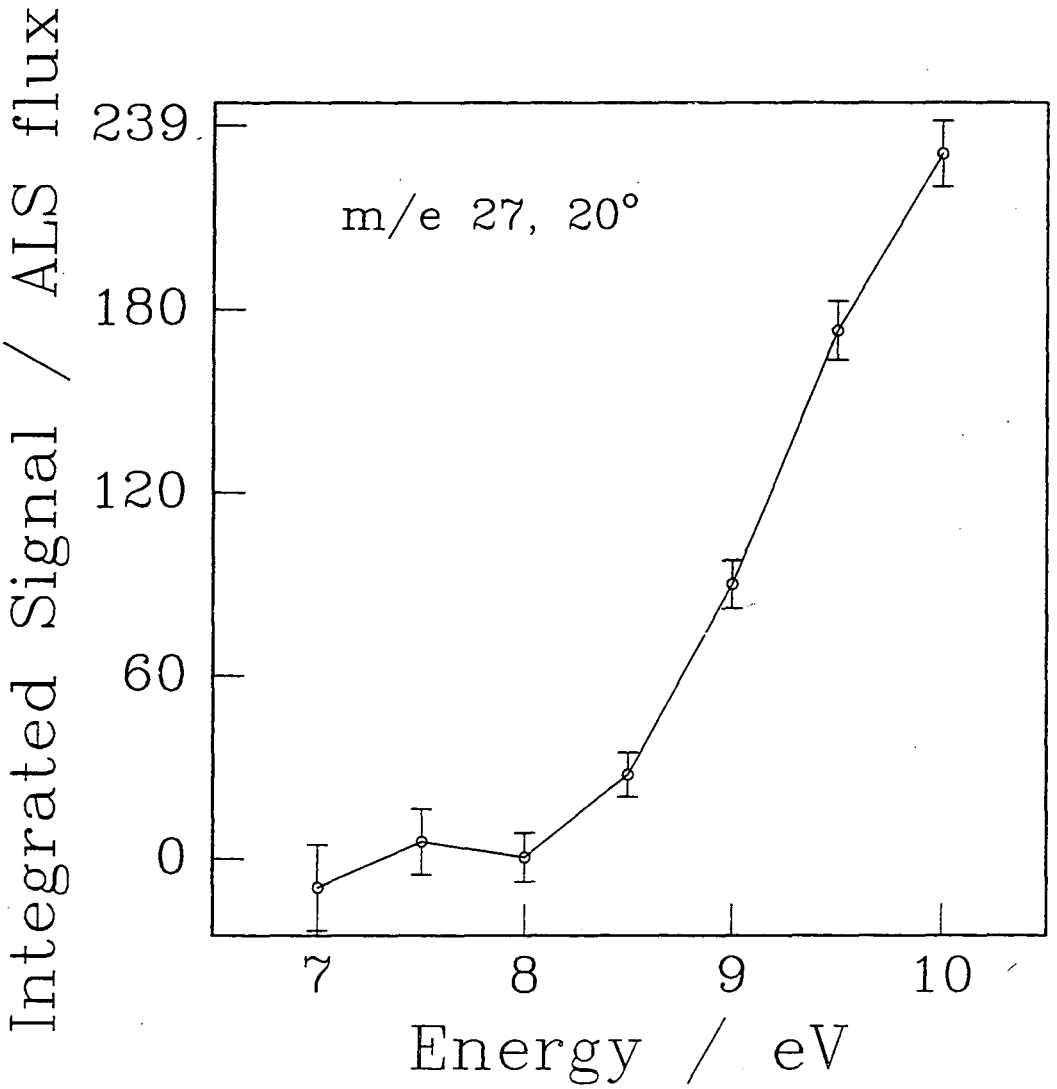
Integrated Signal / ALS flux
239
180
120
60
0
m/e 27, 20°
7
8
9
10
Energy / eV

figure 16

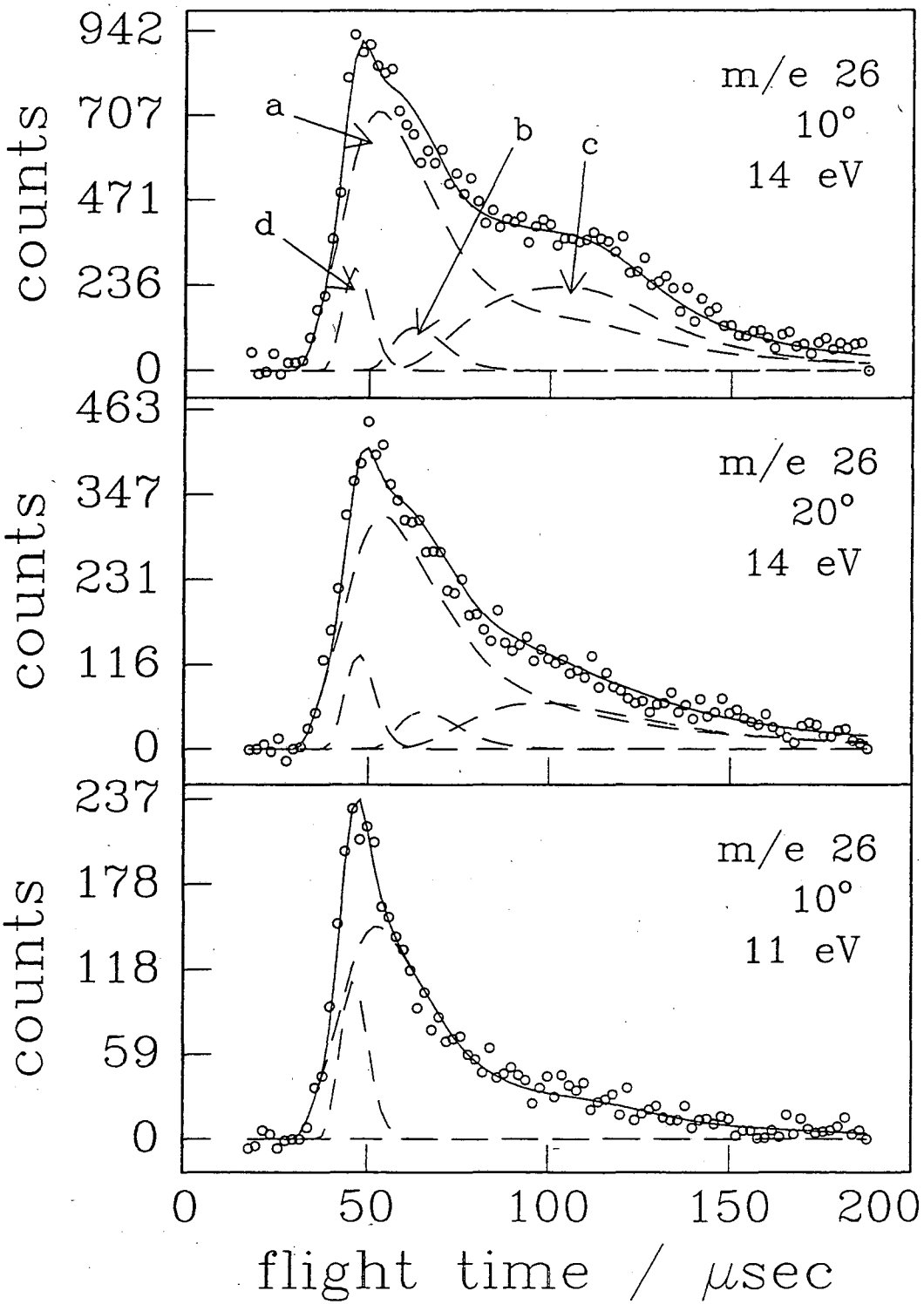
942
707
471
236
0
counts
a
b
c
d
m/e 26
10°
14 eV
463
347
231
116
0
counts
m/e 26
20°
14 eV
237
178
118
59
0
counts
m/e 26
10°
11 eV
0
50
100
150
200
flight time / μsec

figure 17

Ernest Orlando Lawrence Berkeley National Laboratory
One Cyclotron Road | Berkeley, California 94720

Prepared for the U.S. Department of Energy under Contract No. DE-AC03-76SF00098